Progress Report of the Research

Fabrication of PMN-PT Single Crystals by Using the Exaggerated Grain Growth Method

November 2001

School of Materials Science and Eng. and Center for Microstructure Science of Materials, Seoul National Univ., Seoul 151-742, Korea

REPORT DOCUMENTATION PAGE

Form Approved

OMB No. 0704-0188

PLEASE DO NOT RETURN YOUR FORM TO THE ABOVE ADDRESS.

1. REPORT DATE *(DD-MM-YYYY)*	2. REPORT TYPE	3. DATES COVERED *(From - To)*
23-11-2001	Final	

4. TITLE AND SUBTITLE

Fabrication of PMN-PT Single Crystals by Using the Exaggerated Grain Growth Method

5a. CONTRACT NUMBER

F6256200M9140

5b. GRANT NUMBER

5c. PROGRAM ELEMENT NUMBER

6. AUTHOR(S)

Prof. Doh-Yeon Kim

5d. PROJECT NUMBER

5e. TASK NUMBER

5f. WORK UNIT NUMBER

7. PERFORMING ORGANIZATION NAME(S) AND ADDRESS(ES)

Seoul National University
School of Materials Science, Shinlim-Dong, Gwanak-ku
Seoul 151-742
Korea (South)

8. PERFORMING ORGANIZATION REPORT NUMBER

N/A

9. SPONSORING/MONITORING AGENCY NAME(S) AND ADDRESS(ES)

AOARD
UNIT 45002
APO AP 96337-5002

10. SPONSOR/MONITOR'S ACRONYM(S)

AOARD

11. SPONSOR/MONITOR'S REPORT NUMBER(S)

AOARD-004003

12. DISTRIBUTUION/AVAILABILITY STATEMENT

Approved for public release; distribution is unlimited.

13 SUPPLEMENTARY NOTES

14. ABSTRACT

Polycrystalline 65 mole% $Pb(Mg_{1/3}Nb_{1/3})O_3$ -35 mole% $PbTiO_3$ (PMN-PT) specimens were prepared by conventional and spark-plasma sintering. Conventional sintering at 1200°C produced 92% dense specimens, whereas spark-plasma sintering at 900°C produced 99% dense specimens. Addition of slight excesses of Mg accelerated grain growth, but additions of Nb retarded grain growth. In addition, excess Mg decreased dielectric and piezoelectric properties. Grain-growth studies indicated that abnormal grain growth (AGG) occurred when excess Pb was present. The AGG was ascribed to formation of $\Sigma 3$ coincidence-site-lattice and low-angle grain boundaries. Because of reentrant edges appearing at the ends of these boundaries, grain-coarsening rates were significantly enhanced. However, single crystals could not be made by an AGG process.

15. SUBJECT TERMS

Electronic Ceramic, Single crystals

16. SECURITY CLASSIFICATION OF:			17. LIMITATION OF ABSTRACT	18. NUMBER OF PAGES	19a. NAME OF RESPONSIBLE PERSON
a. REPORT	b. ABSTRACT	c. THIS PAGE			Kenneth C. Goretta, Ph.D.
U	U	U	UU	69	19b. TELEPHONE NUMBER *(Include area code)* +81-3-5410-4409

Standard Form 298 (Rev. 8/98)
Prescribed by ANSI Std. Z39.18

Progress Report of the Research

Fabrication of PMN-PT Single Crystals by Using the Exaggerated Grain Growth Method

November 2001

School of Materials Science and Eng. and Center for Microstructure Science of Materials, Seoul National Univ., Seoul 151-742, Korea

To: The Director of AFOSR

This research has been supported from Aug. 2000 to July 2001 (12 months) by AFOSR. Hereby, we submit the progress report.

Nov. 2001

Research Institute: School of Materials Science and Eng. and Center for Microstructure Science of Materials, Seoul National Univ., Seoul 151-742, Korea

Principal Investigator: Prof. Doh-Yeon Kim

Co-investigators: N. M. Hwang and Ho-Yong Lee (Center for Microstructure Science of Materials), and D. Y. Yoon and S.-J. Kang (Korea Advanced Institute of Science and Technology)

Table of contents

1.Introduction

Sintering, a key process for manufacturing of ceramic materials, is a heat-treatment of powder compacts or aggregates to produce a dense body. The driving force for sintering is the reduction of interface free energy of the material system, which can be accomplished by atomic diffusion. The reduction of a solid/vapor interface leads to densification and that of a grain boundary leads to an increase in grain size i.e. grain growth.

During sintering, two types of grain growth are usually observed to occur: (i) normal grain growth (NGG) and (ii) exaggerated or abnormal grain growth (EGG or AGG). During NGG, the average grain size increases continuously without changing the grain size distribution. In EGG, on the other hand, a few large grains develop and grow rapidly at the expense of small matrix grains. The rate of EGG is orders of magnitude higher than that of NGG. Therefore, when EGG is strictly controlled, the single crystal can be grown with a relatively high rate in the solid state. The possibility of growing a single crystal by EGG was already demonstrated in $BaTiO_3$ by our research group [1,2] and in Al_2O_3 by GE researchers [3]. In both cases, the growth rate is comparable to that obtained in the flux or melt growth.

For growing a single crystal by EGG, the number of "nuclei" for EGG should be maintained minimal. For this purpose, the seed for EGG may be provided externally. When the single crystal seed is in contact with a polycrystalline sample, the single crystal seed grows as long as the fine-grained structure in polycrystalline side is maintained. Harmer *et al.* [4] have shown indeed that the $SrTiO_3$ single crystal bonded with

PMN-PT has grown extensively. The growing technique of a single crystal by EGG can be combined with such an externally seeding method. This technique is definitely a low-cost manufacturing method compared with melt growth.

In order to obtain the PMN-PT single crystals by EGG, the following two conditions are expected to be necessary: First, EGG should take place during the heat-treatment of PMN-PT. In the preliminary experiment with PMN-PT, we observed [5] that EGG occurs during sintering when a small amount of excess PbO is added as shown in Fig. 1. Second, the mechanism of EGG in ceramic systems, particularly in PMN-PT, should be understood. Without understanding the mechanism itself, the systematic approach to achieve the final goal would be impossible.

During the first year of this project, we could fabricate the PMN-PT single crystals of $15 \times 12 \times 5$ mm^3 by using EGG. However, we experienced the lack of reproducibility of the high growth rate under the identical processing conditions. Another problem in the PMN-PT single crystal grown by EGG is the relatively high porosity. Improving the reproducibility and controlling the porosity should therefore be the main objectives of the research in future.

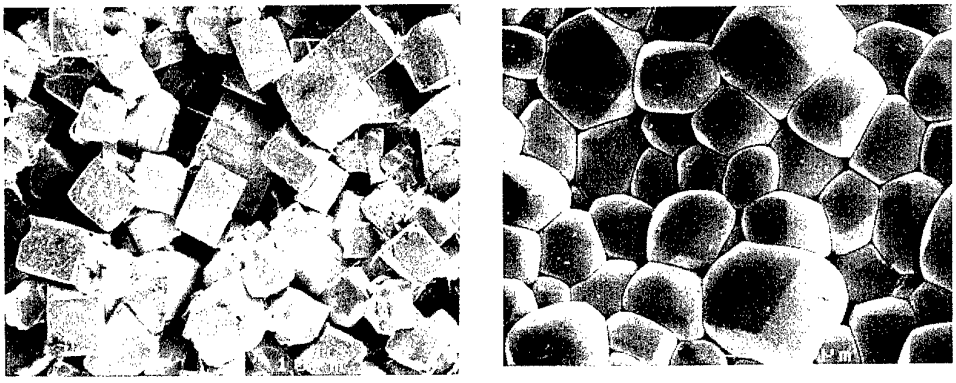

(a) (b)

Fig.1. Interface morphology between two (65)$Pb(Mg_{1/3}Nb_{2/3})O_3$-(35)$PbTiO_3$ (in mole %) specimens (a) with and (b) without excess PbO. The specimen with excess PbO shows the angular grains while the specimen without PbO shows the partially-rounded grains (scales are different).

2. Mechanism of EGG

It is well known that the sintering of a ceramic material such as $BaTiO_3$ is usually carried out in the presence of a small amount of liquid phase either intentionally added or formed by impurities. On the other hand, we recently suggested that EGG in ceramics occurred during sintering in the presence of liquid is a consequence of coarsening controlled by 2D nucleation mechanism [6-16]. When the solid grains are dispersed in a liquid matrix, it has been well established that the interface energy minimization occurs by the dissolution of small grains and reprecipitaion on large ones (Ostwald ripening) [17,18]. The parabolic and cubic coarsening behavior of the average grain sizes were suggested for an interfacial reaction- and diffusion-controlled coarsening process, respectively.

On the other hand, the shape of solid grains is either angular or spherical. For instance, WC grains in Co liquid are angular [6], while W grains in Ni are spherical [19]. In addition, B addition to NbC-Fe alloy has been reported [15] to change the grain shape from angular to spherical. The Wulff theorem [20] predicts that the equilibrium shape of a crystal with a minimum interfacial energy is determined by the anisotropy of the interface energy, γ. Faceted or angular grain shape reflects the presence of a few crystallographic planes with low γ. The spherical grain shape indicates that γ is, more or less, isotropic. Furthermore, the angular and spherical grain shapes indicate that their interface structures are atomically smooth and rough, respectively.

Since the process of grain coarsening occurs at the solid/liquid interface,

the growth mechanism is naturally dependent on the atomic structure of the interface. For spherical grains having an atomically rough interface structure, there would be no energy barrier for atomic attachment at the interface. As a result, the overall coarsening rate is controlled by the diffusion through the liquid matrix. For angular grains, on the other hand, a significant energy barrier is expected for atomic attachment, which results in an interfacial-reaction-controlled coarsening process.

Assuming that the coarsening of angular grains that have an atomically smooth interface structure occurs through a 2-D nucleation and subsequent lateral growth of nuclei, the free energy change associated with nucleation is given by [21]

$$\Delta G = 2\pi R\varepsilon + h\,\pi R^2\,\Delta G_v \qquad (1)$$

where R is the radius of the circular disk shaped nucleus and h is the step edge height. On the other hand, ε is the step edge free energy, which describes the amount of energy necessary to make a unit length of step edge and ΔG_v is the driving force for coarsening. For a grain of a size r, the driving force is [17,18]

$$G_v = 2\,\gamma\,(1/r - 1/r^*) \qquad (2)$$

Here, r^* is a critical size that is neither dissolving nor growing.

From Eq. (1), the energy barrier for 2-D nucleation is

$$\Delta G^*_{2D} = -\pi\,\varepsilon^2 / h\,\Delta G_v \qquad (3)$$

Since the nucleation rate is proportional to $\exp(-\Delta G^*_{2D}/kT)$, the coarsening rate will remain nearly at zero and increase sharply when ΔG_v exceeds a certain value. Therefore, it can be predicted that coarsening is only possible for a few grains that are larger than certain critical size r_c, i.e. for the grains $r > r_c >> r^*$; AGG will occur under this situation. Note that,

for the spherical grains having atomically rough interface the growth is diffusion controlled and the coarsening is possible for all grains $r > r^*$.

Indeed, AGG is observed to occur only when the grains are angular with flat solid/liquid interfaces. WC-Co[6], $BaTiO_3$[7,9,14], NbC-Fe[15], Si_3N_4[10,11], SiC[13], and TaC-TiC-Ni[16] are typical examples of angular grains which exhibit AGG. On the other hand, Eq. (3) indicates that a small change in ΔG^*_{2D} may result in a notable change in coarsening process. The presence of defects which lower ΔG^*_{2D} by acting as heterogeneous nucleation sites has been observed [7,9, 14-16] to greatly increase the coarsening rate. In the case of $BaTiO_3$, the twin-plane reentrant edge (TPRE) provides the site for the lower 2-dimensional nucleation barrier and the grains with a double twin undergo exclusive growth [7,9,14]. It is known that the double twin provides a persistent twin-plane reentrant edge (TPRE).

On the other hand, the formation of grain boundaries during liquid-phase sintering has also been determined to provide reentrant edges. Note that the formation of grain boundaries due to grain coalescence occurs usually because the dihedral angle is not zero in most cases. The probability that two grains will form a grain boundary was investigated by Courtney and Lee [22] for the case of spherical grains. Through the simple relationship between boundary energy and misorientation, they estimated the probability as a function of a few geometrical variables. However, the probability of forming a grain boundary would be difficult to predict for angularl grains. In spite of that, when two randomly oriented cubes collide with each other face-to-face, for instance, the necessary condition for forming a grain boundary ($2\gamma_{sl} < \gamma_{gb}$) would be rather easily satisfied

because the twist grain boundary with relatively low energy can be generated. Note also that two grains may rotate each other to form a low angle or specific orientation during annealing.

The extent of grain boundary formation can be predicted from the dihedral angle. For the system with a dihedral angle of zero, the formation of grain boundaries is impossible. The wetting angle that is experimentally easy to determine may also indicate the extent of grain boundary formation. The lower the wetting angle the lower the solid-liquid interfacial energy, therefore the formation of grian boundaries becomes difficult. In most ceramic material systems, the dihedral angle or wetting angle is larger than zero so that a certain extent of grain boundaries is expected to from.

When a two-dimensional nucleus is formed at a 90° reentrant edge formed by a grain boundary as shown in Fig.2, the ratio of activation energy barrier at the renetrant edge (ΔG^*_{Re}) and that at the surface (ΔG^*_{2D}) is given as

$$\Delta G^*_{Re} / \Delta G^*_{2D} = (\theta - \sin\theta\cos\theta \ / \ \pi \ ) \qquad (4)$$

where θ is the radian contact angle of the two-dimensional nucleus at a reentrant edge. Equation (4) is always smaller than one, indicating that a grain boundary acts as a preferential nucleation site. Considering the two-dimensional nucleation rate on a very large grain, a 10 and 50% reduction in activation energy should result in a ~4.0×10^2 and ~9.7×10^{12} times higher nucleation rate, respectively. The values assumned for caluculation were: $r^* = 1$ μm, h =0.22 nm, $\gamma_{sl} = 0.1$ J/m^2, $\varepsilon / h = 0.02$ J/m^2 and T = 1400 °C. The growth rate of angular grains will therefore greatly enhanced when reentrant edges are present.

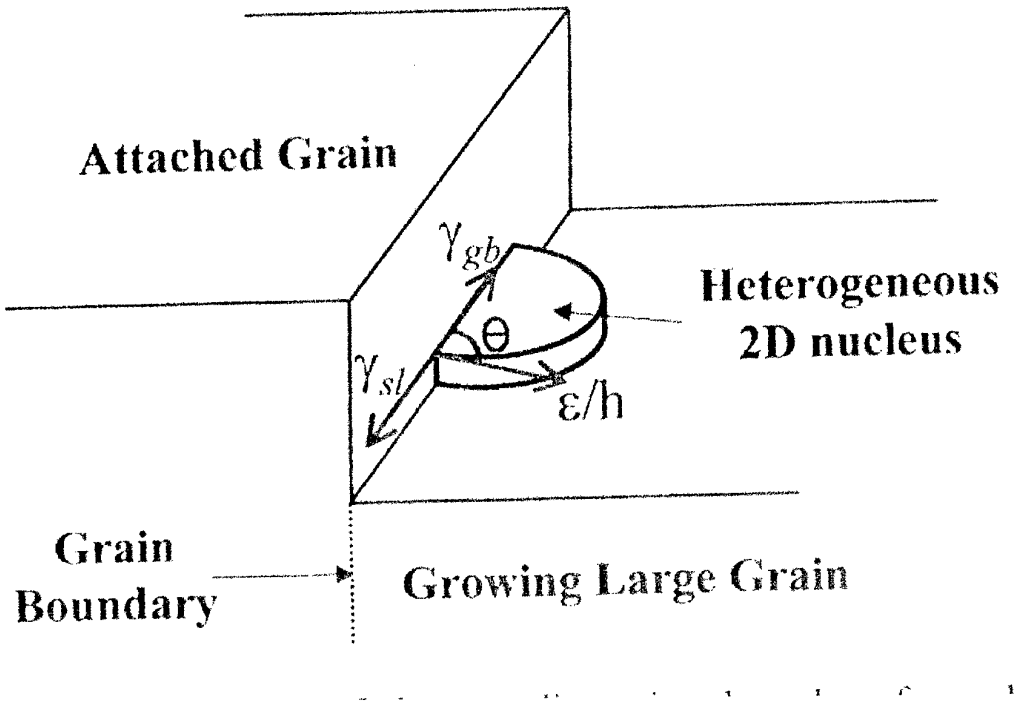

Fig.2 Schematics of the two-dimensional nucleus formed at the reentrant edges made by a grain boundary.

3. Sintering and Grain Growth of PMN-PT

1). Effect of Excess MgO and Nb_2O_5

To obtain a large single crystal of good quality by using EGG, it is necessary to control the grain size, density and chemical homogeneity of the polycrystalline matrix. The maintenance of fine matrix grain size is particularly important because the driving force for single crystal is inversely proportional to the matric grain size. For this purpose, we have checked the effect of small amount of excess MgO and Nb_2O_5, because they affect critically the grain growth behavior. This part of investigation has been summarized in Appendix 1.

2). Mechanism of AGG of PMN-PT Grains

AGG that occurred during the heat-treatment of PMN-35PT ceramics was investigated and it is suggested that AGG is mainly caused by the coalescence of grains and consequent formation of a grain boundary with reentrant edges. In this case, growth is accelerated because the energy barrier for 2-D nucleation is markedly reduced. According to our electron backscattered diffraction (EBSD) or orientation imaging microscopy (OIM) analysis, small grains trapped inside an EGG grain had a low angle or a coincidence site lattice (CSL) boundary. Also, two grains in contact shared a $\Sigma 3$ CSL (or incoherent twin) boundary. The persistent growth of two grains in contact implies that even a single twin provides the persistent re-entrant edge. The large grains turned out to have a penetration twin as shown in Fig 3. This part of study has been the subject of the manuscript submitted for the publication in *J. Am. Ceram. Soc.* (see Appendix 2)

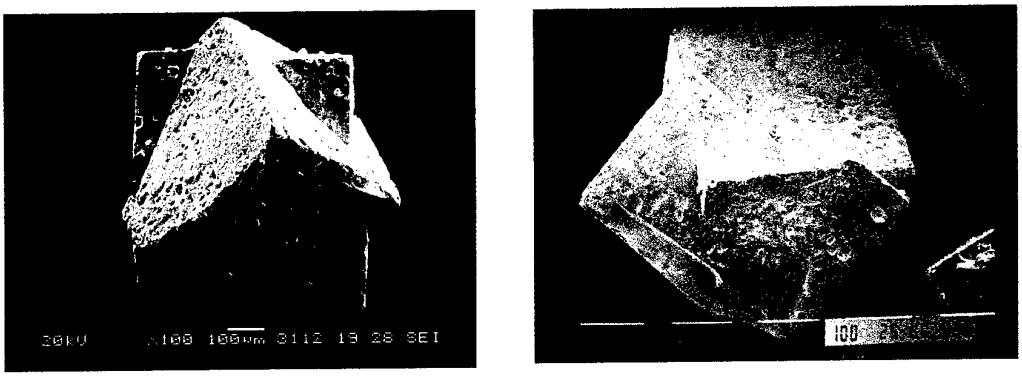

(a) (b)

Fig. 3. Three dimensional morphology of the penetration twin of the PMN-35PT abnormal grains obtained by removal of surrounding matrix grains in the boiling acid after heat-treatment at 1150°C for 20 h.

3). Densification of PMN-PT Ceramics by Spark Plasma Sintering

In fact, it is difficult to obtain a fully dense PMN-35PT without a second pyrochlore phase. Even with the powders prepared by the columbite precursor method [23], both the pyrochlore phase and many pores remain after the low temperature sintering. On the other hand, a dense PMN-PT specimen is still difficult to obtain with high temperature sintering due to a PbO evaporation. In this case, excess PbO is usually added to compensate for the PbO loss and to enhance the material transfer by forming liquid phase during sintering [24,25]. However, such a PbO based liquid remaining at the grain boundaries is known to deteriorate the properties of PMN based ceramics.

To obtain a fully dense and fine-grained material, spark plasma sintering (SPS) was introduced recently and has become widely used [26-28]. Although the mechanism of enhanced densification is not yet clearly

understood, the process itself can be described quite simply: during sintering under relatively low pressure (~30MPa), a pulsed direct current, which generates spark discharge at the voids between the particles, is applied. Through the SPS process, a relatively low temperature and short sintering time (~ a few minutes) is known to be sufficient to achieve a full densification of most ceramics. Therefore, the densification behavior of the PMN-35PT ceramics by SPS was studied. This part is summarized in Appendix 3, and will appear in January 2001 issue of *J. Am. Ceram. Soc.*.

4). Fabrication of PMN-PT Single Crystals

During the sintering of PMN-35PT powder compact with excess PbO, AGG has been observed to occur as shown in Fig. 1. The occurrence of AGG indicates that a PMN-35PT single crystal may also be fabricated. Figure 4 shows the PMN-35PT single crystal obtained. Its size was 1.5 x 1.2 x 0.5 cm^3. In this case, the seed crystal was embedded in the (PMN-35PT)-8PbO powder compact and then heat-treated at 1200 °C for 20 h. As a seed crystal, a $BaTiO_3$ crystal was used. PMN-35PT is observed to grow epitaxially at the surface of the $BaTiO_3$ seed crystal. Note that both PMN-PT and $BaTiO_3$ have same perovskite crystal structure. The same growth result was obtained when the PMN-PT crystal once grown was used as a seed. We consider that this simple method using AGG will provide a break-through in the fabrication of PMN-PT single crystals.

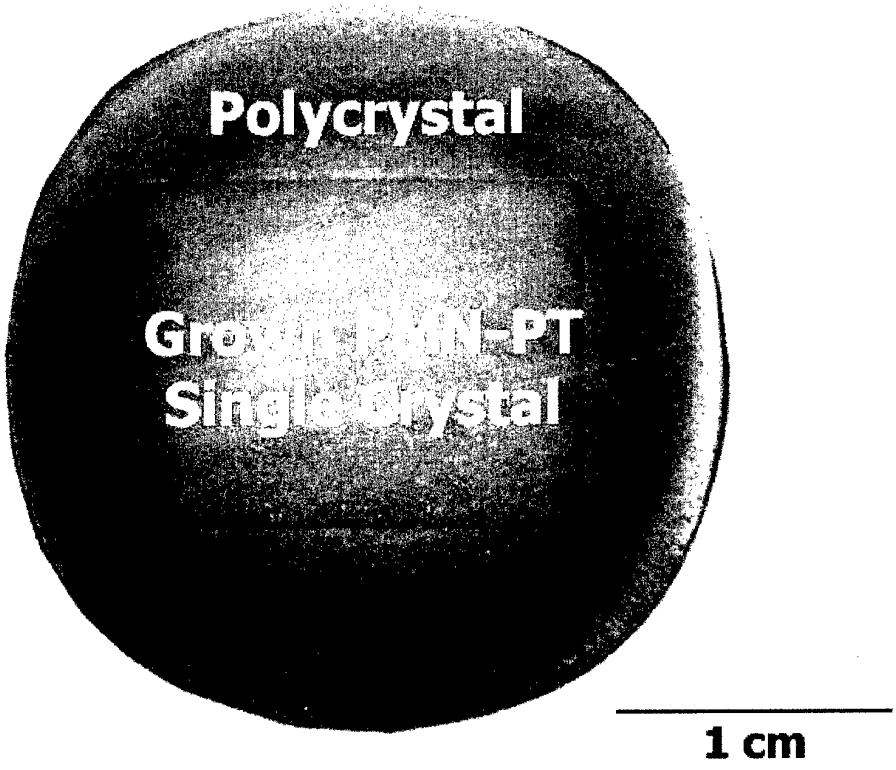

Fig. 4. PMN-PT single crystal grown in polycrystalline matrix. The seed grain has grown by consuming the matrix grains.

4. Further works – Porosity Minimization and Enhancement of Reproducibility

1). Porosity

PMN-PT single crystals obtained as shown in Fig.4 are characterized by the relatively high porosity. The pores are trapped as a result of fast interface migration. Note that the polycrystalline matrix of PMN-PT has relatively high porosity in conventional heat-treatment. These pores in single crystal are critically harmful for optical applications. When the crystals are used as an actuator, on the other hand, the high toughness is required. For this purpose, the PMN-PT single crystals with uniformly distributed pores of moderate size are likely to have an advantage in toughness compare to the melt-grown single crystals with zero porosity. However, the crystals we obtained were so porous that they do not seem to have a practical value.

Therefore, the porosity control is an important subject. In order to reduce the porosity level, we tried to make the PMN-PT single crystals by two different methods: conventional sintering and spark plasma sintering (SPS). As shown in Fig. 5, SPS has a pronounced effect on the reduction of pores in the single crystal. By SPS treatment at 900°C for 2 min under 30 MPa, the relative density could be increased up to 99.5%. Although the porosity decreased markedly, the growth rate of the seed grain did not decrease. We observed, however, that the processing window for single crystal fabrication is very narrow. More systematic studies should be carried out in the next year of this project.

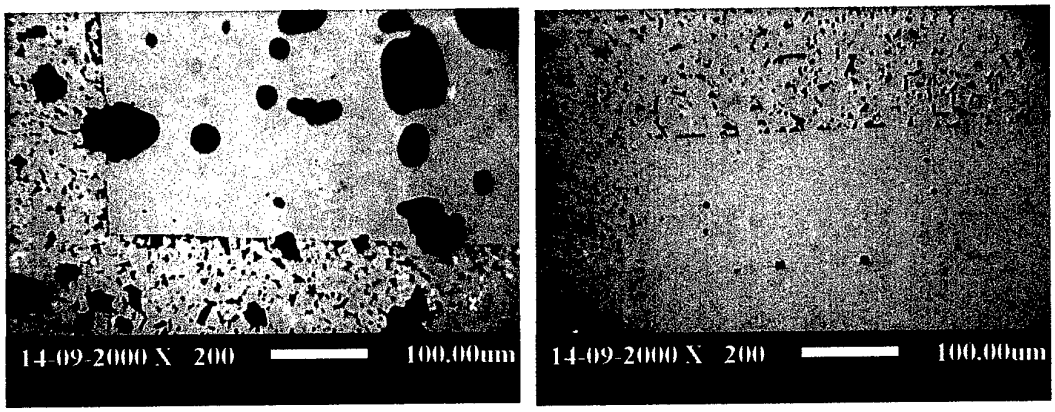

(a) Conventional Sintering (b) Spark Plasma Sintering

Fig. 5 Comparison of the PMN-PT single crystals grown by EGG: (a) conventional sintering and (b) spark plasma sintering.

2). Reproducibility

In the first year of the project, we tried to understand EGG behavior of PMN-PT ceramics and to make a large PMN-PT single crystal. Most important problem that we encountered during research is that reproducibility of the expermental result is relatively low. This is mainly due to too many variables in processing from powder preparation to heat-treatment for sintering and crystal growth. In fact, to examine the effect of all the relevant variables simultaneoulsy, too many experiments are required. For instance, the total number of experiments for four variables with three levels would be 3^4, i.e. 81. In order to overcome this problem, we tried to identify the parameters related to the reproducibility by the Taguchi method using the L_{18} orthogonal array as shown in Table I. The experiments are now carrying out and the optimum parameters will be determined in near future.

Table 1. Experimental layout using L18 orthogonal array

Exp. #	Precursor	PbO	MgO	Milling	PMN-PT Cal.T ℃	PVA (wt%)	Embed. Powder	Sinter. T (℃)
1	MgNb Columbite	After 5mol%	0	planetary 2h	750	0	Same	1100
2	MgNb Columbite	After 5mol%	2mol%	planetary 30min	800	1	PZ	1150
3	MgNb Columbite	After 5mol%	5mol%	ball	850	0.5	PZ+PbO	1200
4	MgNb Columbite	0	0	planetary 2h	800	1	PZ+PbO	1200
5	MgNb Columbite	0	2mol%	planetary 30min	850	0.5	Same	1100
6	MgNb Columbite	0	5mol%	ball	750	0	PZ	1150
7	MgNb Columbite	Before 5mol%	0	planetary 30min	750	0.5	PZ	1200
8	MgNb Columbite	Before 5mol%	2mol%	ball	800	0	PZ+PbO	1100
9	MgNb Columbite	Before 5mol%	5mol%	planetary 2h	850	1	Same	1150
10	MgTiNb Columbite	After 5mol%	0	ball	850	1	PZ	1100
11	MgTiNb Columbite	After 5mol%	2mol%	planetary 2h	750	0.5	PZ+PbO	1150
12	MgTiNb Columbite	After 5mol%	5mol%	planetary 30min	800	0	Same	1200
13	MgTiNb Columbite	0	0	planetary 30min	850	0	PZ+PbO	1150
14	MgTiNb Columbite	0	2mol%	ball	750	1	Same	1200
15	MgTiNb Columbite	0	5mol%	planetary 2h	800	0.5	PZ	1100
16	MgTiNb Columbite	Before 5mol%	0	ball	800	0.5	Same	1150
17	MgTiNb Columbite	Before 5mol%	2mol%	planetary 2h	850	0	PZ	1200
18	MgTiNb Columbite	Before 5mol%	5mol%	planetary 30min	750	1	PZ+PbO	1100

References

1. Y. S. Yoo, M. K. Kang, J. H. Han, H. Kim, and D. Y. Kim, *J. Eur. Ceram. Soc.*, **17**, 1725-27 (1997).
2. H. Y. Lee, J. S. Kim, and D. Y. Kim, *J. Eur. Ceram. Soc.* **20.** 1595-97 (2000)
3. C. Scott, J. Strok, and L. Levinson, U.S. Pat. No. 5,549,746 (1996).
4. M. P. Harmer, presented in the Workshop SSCG, Feb.17, 1999.
5. H. Y. Lee, H. M. Chan, and M. P. Harmer, *J. Kor. Ceram. Soc.*, **35**, 905 (1998).
6. Y. J. Park, N. M. Hwang, and D. Y. Yoon, *Metall. Mater. Trans.*, **27A**, 2809-19 (1996).
7. M.-K. Kang, Y.-S. Yoo, D.-Y. Kim, and N. M. Hwang, *J. Am. Ceram. Soc.*, **83**[2], 385-90 (2000).
8. S.-K. Kwon, S.-H. Hong, D.-Y Kim, and N. M. Hwang, *J. Am. Ceram. Soc.*, **83**[5], 1247-52 (2000).
9. Y.-S. Yoo, H. Kim, and D.-Y Kim, *J. Euro. Ceram. Soc.*, **17**, 805-11 (1997).
10. S.-J. L. Kang, and S.-M. Han, *Mater. Res. Bull.*, **20**, 33-37 (1995)
11. S.-H. Rhee, J. D. Lee, and D.-Y. Kim, *Mater. Lett.*, **32**, 115-120 (1997).
12. H.-H. Yoon, and D.-Y Kim, *Mater. Lett.*, **20**, 293-97 (1994).
13. Y.-W. Kim, J.-Y. Kim, S.-H. Rhee, and D.-Y. Kim, *J. Euro. Ceram. Soc.*, **20**, 945-49 (2000).
14. M.-G. Kang, D.-Y. Kim, H.-Y. Lee, and N. M. Hwang, *J. Am. Ceram. Soc.*, **83**[12], 3202-204 (2000).
15. K.-S. Oh, J.-Y. Jun, D.-Y. Kim, and N. M. Hwang, *J. Am. Ceram. Soc.*, **83**[12], 3117-20 (2000).
16. K. Choi, J.-W, Choi, D.-Y., Kim, and N. M, Hwang, *Acta mater.*, **48**, 3125-29 (2000).
17. G. W. Greenwood, *Acta metall.*, **4[5]**, 243-48 (1956).
18. R. D. Vengrenovitch, *Acta metall.*, **30**, 1079-86 (1982).
19. D. N. Yoon, and W. J. Huppmann, *Acta metall.*, **27**, 693-98 (1979).
20. C. Herring, *Phys. Rev.*, **82[1]**, 87-93 (1951).
21. J. M. Howe, *Interfaces in Materials*, pp83-86, John Wiley & Sons, New York, 1997.
22. T. H. Courtney, and J. K. Lee, *Metall. Trans.*, **11A**, 943-49 (1980).
23. S. L. Swartz and T. R. Shrout, *Mater. Res. Bull.*, **17** 1245-50 (1982).
24. Z.-G. Ye, P. Tissor, and H. Schmid, *Mater. Res. Bull.*, **25** 739-48 (1990).

25. B. Jaffe, W. R. Cook, Jr., and H. Jaffe, *Piezoelectric ceramics*; p.117. Academic Press, London, U.K., 1971
26. D. S. Perera, M. Tokita, and S. Moricca, *J. Eur. Ceram. Soc.,* **18** 401-04 (1998).
27. T. Takeuchi, M. Tabuchi, H. Kageyama and Y. Suyama, *J. Am. Ceram. Soc.,* **82** [4] 939-43 (1999).
28. J. Hong, L. Gao, S.D.D.L. Torre, H. Miyamoto, and K. Miyamoto, *Mater. Lett.,* **43** 27-31 (2000).
29. G. Taguchi, *System of Experimental Design*, pp. 169-76, Vols 1 and 2, ed. D. Clausing, UNIPUB/Kraus, New York, (1987).

Appendix 1

Effect of Excess MgO and Nb_2O_5 on the Microstructure and Properties of PMN-35PT Ceramics

Jong-Keuk Park and Doh-Yeon Kim
School of Materials Science and Engineering and Center for Microstructure Science of Materials, Seoul National Univ., Seoul 151-744, Korea

Nong M. Hwang
Korea Research Inst. of Standards and Science, Daedok 305-600, Korea

Jong-Bong Lee and Ho-Yong Lee
Division of Metallurgical and Materials Engineering, Sunmoon University, Chungnam, Asan 336-840, Korea

---

Supported by the Ministry of Science & Technology of Korean Government through National Creative Research Initiatives and Asian Office of Aerospace Research and Development (AOARD-00-4003).

Abstract

The changes in microstructure, dielectric and piezoelectric properties of PMN-35T ceramics by the addition of excess MgO and Nb_2O_5 have been investigated. The addition of a small amount of MgO accelerated grain growth during sintering but Nb_2O_5 addition retarded it. Excess Nb_2O_5 also drastically decreased the dielectric and piezoelectric properties.

Introduction

$Pb(Mg_{1/3}Nb_{2/3})O_3$ (PMN) and $PbTiO_3$ (PT) solid solutions have been investigated extensively for various applications such as actuators and ultrasonic transducers.[1] In PMN-xPT(x in mol%), a morphotropic phase boundary (MPB) separating pseudo-cubic and tetragonal phases is known to exist at approximately x=35.[2,3] At this MPB composition of PMN-35PT, particularly when the specimens are in single crystals, very exceptional dielectric and piezoelectric properties are reported to appear.[4,5]

Although the single crystals are usually obtained by high temperature melt technique, there is a critical limitation in processing of PMN-PT because a chemical homogeneity throughout the crystal is difficult to achieve. An extremely low rate of crystal growth is another limitation. For these reasons, a more convenient single crystal fabrication method, which involves embedding a seed crystal in a polycrystalline precursor, has been reported.[6,7] During heat-treatment, the seed crystal may grow by a capillary driving force and the small matrix grains are consumed.

To obtain a large single crystal of good quality by this process, it is necessary to control the grain size, density and chemical homogeneity of the polycrystalline matrix. The maintenance of a fine matrix grain size is particularly important because the driving force for single crystal growth is inversely proportional to the matrix grain size. In this respect, it is important to check the microstructural evolution during the sintering of PMN-PT ceramics. Recently, low temperature reactive sintering technique was proposed for obtaining a fully dense specimen.[8]

In this investigation, a small amount of excess MgO or Nb_2O_5 was added to the PMN-35PT and their effects on grain growth during heat-treatment were checked. Both the dielectric and piezoelectric properties of the resultant PMN-35PT ceramics were also determined. It is suggested that excess MgO or Nb_2O_5 should be carefully controlled to fabricate a capillary driven PMN-PT single crystal because they affect critically the grain growth behavior.

Experimental Procedures

The PMN-35PT powders were prepared by the columbite precursor technique.[9] The $MgNb_2O_6$ precursor was prepared with $(MgCO_3)_4Mg(OH)_25H_2O$ (Hayashi Pure Chemical Industries, Osaka, Japan) and Nb_2O_5 (Aldrich Chemical Co., Milwaukee, WI, U.S.A.). The powders were weighed and ball-milled for 24 h using a polyethylene jar with ethanol and zirconia balls. After drying, the powders were calcined at 1100℃ for 4 h in air. The PMN-35PT powders were then prepared with PbO, TiO_2 (Both from Aldrich Chemical Co., Milwaukee, WI, U.S.A.) and the $MgNb_2O_6$ that was obtained previously. The powder mixture was ball-milled for 24 h using a polyethylene jar with ethanol and zirconia balls. After drying, the powders were calcined at 850℃ for 4 h in air. The calcined powders were ball-milled again for 12h. The complete formation of perovskite was confirmed by X-ray diffractometry (XRD).

The PMN-35PT powders obtained were again mixed with a 2 mol% excess MgO or a 0.5 mol% excess Nb_2O_5. These amounts correspond to the solubility limit for MgO[10] and Nb_2O_5. For Nb_2O_5, the solubility limit was determined through preliminary experiments. The powders were compacted uniaxially at low pressure into cylindrical specimens of 1 cm in diameter and then pressed hydrostatically at 150 MPa. The compacts were sintered at 1200℃ for 1 h and $PbZrO_3$ powder was used as an atmospheric powder to prevent PbO evaporation. The heating rate was 5℃/min and the specimens were furnace-cooled to room temperature.

For microstructure observation using a scanning electron microscope

(SEM), the cylindrical specimens were sectioned along the diameter and polished surfaces were thermally etched at 1000℃ for 30 min. The average grain size was determined by multiplying 1.775 to the mean intercept length.[11] Dielectric and piezoelectric properties were determined by using 0.5-mm thick disc type samples with flat and parallel surfaces. Silver pastes were painted on both sides of the samples and then heat-treated at 600℃ for 30 min. For low-field measurements using resonance technique[12], the samples were poled by applying 40kV/cm at room temperature. The temperature dependence of the dielectric constant was measured at 1kHz using an impedance analyzer (HP 4192A). The planar coupling factor (k_p), transverse coupling factor (k_{31}) and piezoelectric coefficient (d_{31}) were also measured by an impedance analyzer (Solartron 1260). The d_{33} value was determined by using PIEZO d_{33} meter (MODEL ZJ-3D, Institute of Acoustics Academia Sinica, China).

Results and Discussion

Figure 1(a) is the microstructure of the PMN-35PT specimen without any excessive MgO or Nb_2O_5. The relative density and average grain size were determined to be about 96.5% and 6 μm, respectively. On the other hand, Fig. 1(b) and (c) show the microstructures of the specimen containing a 2.0 mol% excess MgO and a 0.5 mol% excess Nb_2O_5, respectively. In these specimens, densification was further enhanced; 98.8% of the relative density was achieved in both cases. However, the grain sizes were very different from each other. Compared to the specimen shown in Fig. 1(a), the grain size increased to about 8 μm by MgO addition, but decreased to about 2 μm by Nb_2O_5 addition. The formation of second phase such as pyrochlore was not detected in any of the specimens.

Figure 2 shows the temperature dependence of dielectric constant measured at 1kHz. The sharp paraelectric-ferroelectric phase transition observed to occur in all specimens at around 155℃ indicates that they are close to the tetragonal phase region near the MPB.[2,3] The MgO added specimen showed the highest peak value of 53,800, while the Nb_2O_5 added specimen showed the lowest peak value of 23,900. For the PMN-35PT specimen without any excessive constituents, it was 50,300.

The piezoelectric properties of the specimens are summarized in Table I. Compared to the simple PMN-35PT specimen, the planar coupling factors (k_p), transverse coupling factors (k_{31}) and piezoelectric coefficients (d_{31}, d_{33}) were all observed to increase by the addition of MgO. On the other hand, all of these properties decreased by the addition of Nb_2O_5.

Particularly for the d_{31} and d_{33}, the Nb_2O_5 added specimen exhibited much lower values when compared to the other specimens.

For PMN-based ceramics free from second phases[14,15], their dielectric and piezoelectric properties are known to mainly depend on the grain size and density. In this regard, the change in material properties due to MgO or Nb_2O_5 addition is expected to be mainly due to the differences in the grain size of the specimens. Note that the PMN-35PT specimens with excess MgO or Nb_2O_5 addition had the same level of relative density. According to the series mixing theory for diphasic systems, the relative dielectric constant of polycrystalline ceramics can be expressed as[10]

$$\frac{1}{\varepsilon_s} = \frac{1}{\varepsilon_g} + \frac{t}{D\varepsilon_{gb}} \qquad 1)$$

where ε_s, ε_g and ε_{gb} are dielectric constant of the specimen and those of the grain and the grain boundary phase, respectively. On the other hand, t and D are the thickness of the grain boundary layer and the grain size, respectively. Therefore, the ε_s value is predicted to increase as the grain size increases, as observed in this experiment.

For the PMN[10] and 90PZMN-10PT[13] systems, indeed, the increase in dielectric constant with MgO addition was explained in terms of an increase in grain size. In this respect, the decrease in dielectric constant with the addition of Nb_2O_5 can also be attributed to the fine grain size of the specimen. When Nb_2O_5 was added over the solubility limit, the dielectric constant was observed to decrease due to the formation of a pyrochlore phase.[16] In this experiment, however, both ε_g and ε_{gb} as well as t are also expected to vary with the addition of either MgO or Nb_2O_5, therefore, details of the mechanism responsible for the property variation

are presently unknown.

Conclusions

In PMN-35PT ceramics, the grain size, dielectric and piezoelectric properties were observed to increase with a small amount of excess MgO, but decrease with excess Nb_2O_5. These results show that a small change in composition influences both the microstructure and material properties of PMN-35PT ceramics. Careful control of the excess constituents is necessary to produce a capillary driven PMN-PT single crystal.

References

1. K. Uchino, "Electrostrictive Actuators: Materials and Applications," *Am. Ceram. Soc. Bull.*, **65[4]** 647-52 (1986).
2. S. W. Choi, T. R. Shrout, S. J. Jang and A. S. Bhalla, "Dielectric and Pyroelectric Properties in the $Pb(Mg_{1/3}Nb_{2/3})O_3$-$PbTiO_3$ System," *Ferroelectrics,* **100** 29-38 (1989)
3. T. R. Shrout, Z. P. Chang, N. Kim and S. Markgraf, " Dielectric Behavior of Single Crystal near the (1-x)$Pb(Mg_{1/3}Nb_{2/3})O_3$-(x)$PbTiO_3$ Morphotropic Phase Boundary," *Ferroelectrics Letters,* **12** 63-69 (1990)
4. S.-E. Park and T. R. Shrout, " Ultrahigh Strain and Piezoelectric Behavior in Relaxor Based Ferroelectric Single Crystal," *J. Appl. Phys.*, **82[4]** 1804-11 (1997).
5. S.-E. Park and T. R. Shrout, "Characteristics of Relaxor-Based Piezoelectric Single Crystals for Ultrasonic Transducer," *IEEE Trans on Ultasonics, Ferroelectrics, and Frequency Control Special Issues on Ultrasonic Transducer,* **44[5]** 1140-46 (1997).
6. T. Li, A.M. Scotch, H.M. Chan, M.P. Harmer, S.-E. Park, T.R. Shrout and J.R. Michael, "Single Crystals of $Pb(Mg_{1/3}Nb_{2/3})O_3$-35 mol% $PbTiO_3$ from Polycrystalline Precursors," *J. Am. Ceram. Soc.*, **81[1]** 244-48 (1998)
7. A. Khan, F.A. Meschke, T. Li, A.M. Scotch, H.M. Chan and M.P. Harmer, "Growth of $Pb(Mg_{1/3}Nb_{2/3})O_3$-35 mol% $PbTiO_3$ Single Crystals from (111) Substrates by Seeded Polycrystal Conversion," *J. Am. Ceram. Soc.*, **82[11]** 2958-62 (1999)
8. S. Kwon, E. M. Sabolsky and G. L. Messing, "Low-Temperature Reactive Sintering of 0.65PMN-0.35PT," *J. Am. Ceram. Soc.*, **84[3]** 648-50 (2001)
9. S. L. Swartz and T. R. Shrout, "Fabrication of Perovskite Lead Magnesium Niobate," *Mater. Res. Bull.*, **17** 1245-50 (1982).
10. H.-C. Wang and W. A. Schulze, "The Role of Excess Magnesium Oxide or Lead Oxide Determining the Microstructure and Properties of Lead Magnesium Niobate," *J. Am. Ceram. Soc.*, **73[4]** 825-32 (1990).
11. J.-H. Han and D. -Y. Kim, " Analysis of the Proportionality Constant Correlating the Mean Intercept Length to the Average Grain Size," *Acta Metall. mater.*, **43[8]** 3185-88 (1995).
12. "IRE standards on piezoelectric crystals: Measurements of piezoelectric ceramics, 1961", *Proc. IRE,* **49**, 1161-69 (1961)
13. H. M. Jang, K.-M. Lee and M.-H. Lee, "Stabilization of Perovskite

Phase and Dielectric Properties of $Pb(Zn,Mg)_{1/3}Nb_{2/3}O_3$-$PbTiO_3$ Ceramics Prepared by Excess Constituent Oxides," *J. Mater. Res.*, **9[10]** 2634-44 (1994).

14. P. Papet, J. P. Dougherty and T. R. Shrout, " Particle and Grain Size Effects on the Dielectric Behavior of the Relaxor Ferroelectric $Pb(Mg_{1/3}Nb_{2/3})O_3$," *J. Mater. Res.*, **5[12]**, 2902-09 (1990).
15. S.F. Wang, U. Kumar, W. Huebner, P. Marsh, H. Kankul and C.G. Oakley, "Grain Size Effect on the Induced Piezoelectric Properties of 0.9PMN-0.1PT Ceramic,"; pp.148-151 in *Proceedings of the 8th IEEE International Symposium on Applications of Ferroelectrics*, 1992.
16. J. Chen and M. P. Harmer, " Microstructure and Dielectric Properties of Lead Magnesium Niobate-Pyrochlore Diphasic Mixtures," *J. Am. Ceram. Soc.*, **73[1]** 68-73 (1990).

Table I. Piezoelectric properties of the specimens obtained.

Compositions	k_p	k_{31}	d_{31} (pc/N)	d_{33} (pc/N)
PMN-35PT	0.65	0.38	-244	480
PMN-35PT-2.0 mol% MgO	0.68	0.40	-262	545
PMN-35PT-0.5 mol% Nb_2O_5	0.59	0.35	-210	425

List of figure captions.

Fig. 1 Microstructures of the PMN-35PT specimens sintered at 1200°C for 1 h; (a) without any excessive constituents (b) with 2.0 mol% excess MgO and (c) with 0.5 mol% excess Nb_2O_5.

Fig. 2. Dielectric constants at 1kHz for the PMN-35PT specimens sintered at 1200°C for 1 h.

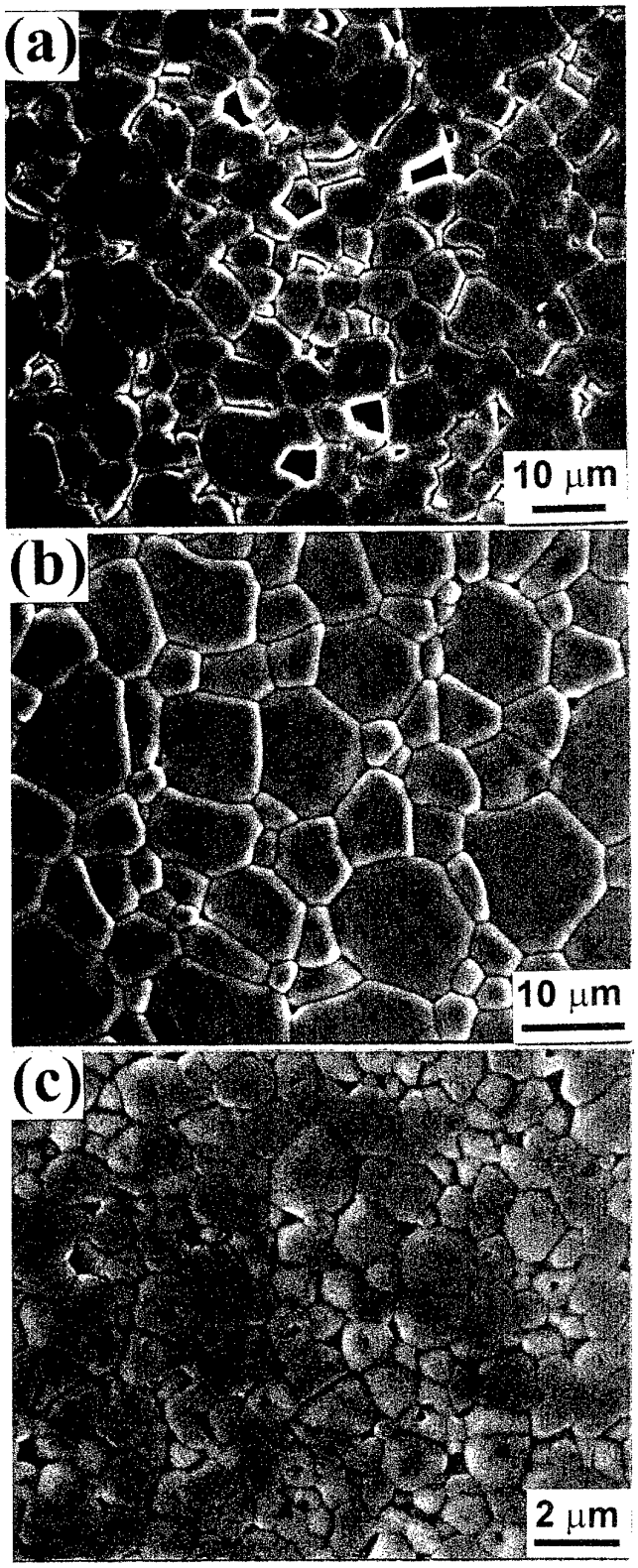

Fig. 1 Microstructures of the PMN-35PT specimens sintered at 1200°C for 1 h; (a) without any excessive constituents (b) with 2.0 mol% excess MgO and (c) with 0.5 mol% excess Nb_2O_5.

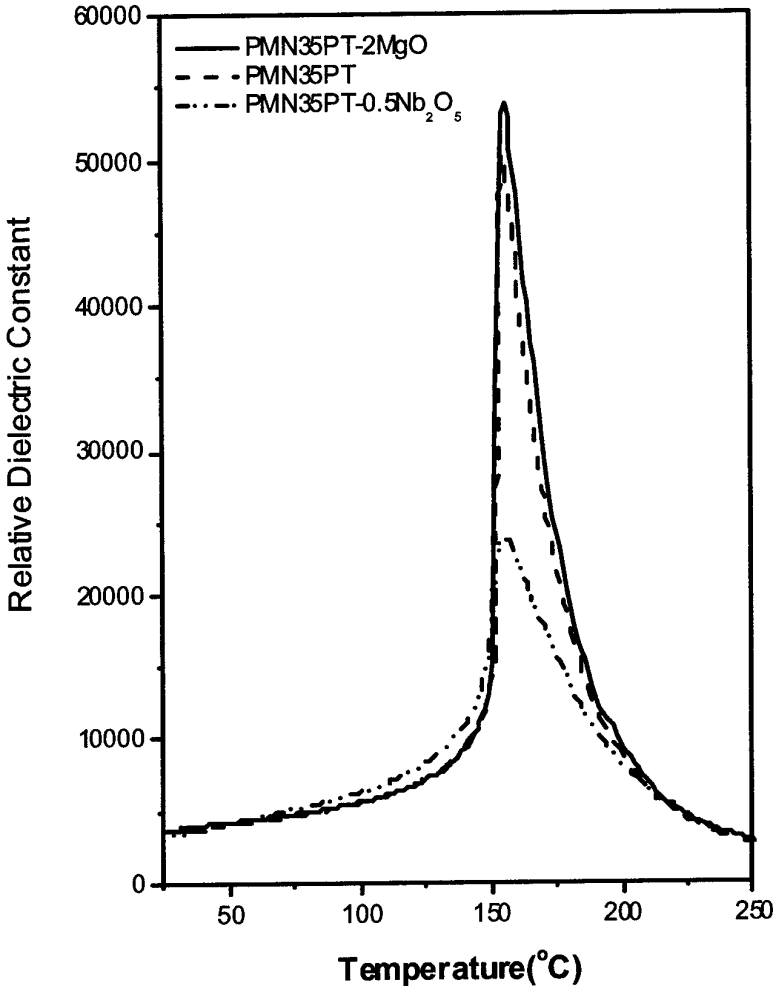

Fig. 2. Dielectric constants at 1kHz for the PMN-35PT specimens sintered at 1200°C for 1 h.

Appendix 2

Effect of Grain Coalescence on the Abnormal Grain Growth of $Pb(Mg_{1/3}Nb_{2/3})O_3$-35mol% $PbTiO_3$ Ceramics

Ui-Jin Chung , Jong-Keuk Park and Doh-Yeon Kim
Center for Microstructure of Materials & School of Materials Science & Eng., Seoul National University, Seoul 151-742, Korea

Nong-Moon Hwang
Korea Research Inst. of Standards and Science, Taejon 305-606, Korea

Ho-Yong Lee
Division of Metallurgical and Materials Eng., Sunmoon Univ., Asan 336-840, Korea

---

Supported by the Ministry of Science & Technology of Korean Government through National Creative Research Initiatives and Asian Office of Aerospace Research and Development (AOARD-00-4003).

Abstract

Abnormal grain growth (AGG), which occurred during the heat-treatment of $Pb(Mg_{1/3}Nb_{2/3})O_3$-35 mol% $PbTiO_3$ (PMN-35PT) with excess PbO, was investigated. AGG has been suggested to be the consequence of grain coalescence that results in the formation of $\Sigma 3$ coincidence site lattice and low angle grain boundaries. Due to reentrant edges appearing at the ends of these boundaries, the coarsening rate of grains was significantly enhanced and AGG occurred.

I. Introduction

Recently it has been reported[1,2] that single crystals of $Pb(Mg_{1/3}Nb_{2/3})O_3$ –35 mol% $PbTiO_3$ (hereafter referred to as PMN-35PT) have excellent electromechanical properties. Many studies have been conducted to obtain single crystals of relaxor-PT by conventional solution growth method using Pb-based fluxes.[2-4] However, compositional uniformity throughout the crystal is difficult to achieve using this technique.

On the other hand, it has been suggested that the PMN-35PT crystals can also be produced by embedding a seed crystal in a polycrystalline matrix.[5,6] During heat-treatment, the seed crystal grows consuming the matrix grains. Note that the size of the matrix grains should be kept small for this process because the growth rate of the seed crystal is proportional to the size difference. In particular, abnormal grain growth (AGG) should be prevented; otherwise the growth of the seed crystal would be severely retarded.

In this study, the AGG that occurred during the heat-treatment of PMN-35PT ceramics was investigated and it is suggested that AGG can be caused by the coalescence of grains and the consequent formation of grain boundaries with reentrant edges. For angular grains with faceted solid-liquid interfaces as in PMN-35PT, coarsening is known to occur by 2-dimensional (2-D) nucleation and lateral growth mechanism.[7-11] In this case, growth is accelerated when reentrant edges are formed because the energy barrier for 2-D nucleation is markedly reduced. This has already been observed in $BaTiO_3$,[12-15] Al_2O_3,[16] NbC-Fe[17] and TaC-TiC-Ni.[18]

II. Experimental Procedure

The columbite precursor method was used for powder preparation. The $MgNb_2O_6$ precursor was prepared with $(MgCO_3)_4$鼠$g(OH)_2$ $5H_2O$ (extra pure reagent, Hayashi Pure Chemical Industry Ltd., Osaka, Japan) and Nb_2O_5 (99.9% , Aldrich Chemical Co., Milwaukee, WI, U.S.A..). The powders were weighed and ball-milled for 24 h in ethanol. After drying, the powders were calcined at 1100°C for 4 h. The PMN-35PT powders were then prepared with PbO (99.9%, Aldrich) and TiO_2 (99.9%, Aldrich). The resulting powders were again ball-milled and calcined at 800°C for 2 h. After calcination, a 10 mol% excess of PbO was added and ball-milled again. X-ray diffraction confirmed the resultant powders to be the mixture of perovskite and PbO phases.

The obtained powders were cold isostatically pressed at 100 MPa and the compacts were heat-treated extensively at 1200°C for 100 h to induce AGG. The compacts were placed in a tightly closed alumina crucible and covered with the same PMN-35PT powders to minimize PbO evaporation. The specimen was polished and an optical as well as scanning electron microscopy was used for microstructure observation. Energy dispersive spectroscopy (EDS) analysis was also used for microchemical analysis. The grain orientation was determined using an electron back scattered diffraction (EBSD) (Oxford/Link Opal, England).

III. Results and Discussions

Fig. 1 shows the microstructure of a specimen obtained after the heat-treatment at 1200°C for 100 h. Abnormally grown large grains up to ~1000 μm in size can be clearly discerned. Note that many pores are trapped inside these abnormal grains probably due to nondiffusable gas such as N_2. The pores are expected to grow with heat-treatment as in the case of the liquid-phase sintering of MgO-$CaMgSiO_4$.[19] The high vapor pressure of PbO may also lead to the increase in porosity with heat-treatment. On the other hand, Fig. 2 shows the microstructure of the matrix grains. They are dispersed in a PbO-rich liquid matrix but form a skeletal structure by joining with neighboring grains. The average size of the matrix grains was determined to be 12.3 μm by the linear intercept method.[20] EDS analysis showed that the matrix liquid phase was composed mainly of PbO (~92%).

As can be seen from Fig. 1 and 2, the PMN-PT grains are angular with sharp corners and straight edges regardless of their size. Fig. 3 shows the three-dimensional shape of the matrix grains obtained after leaching out the liquid phase by a solution of 20% HNO_3 plus 0.5% HF. From this observation and the pseudocubic crystal structure of PMN-35PT,[2] a cube bounded by (100) planes is believed to be its equilibrium crystal shape in a PbO-rich liquid. This implies that the solid-liquid interface structure is atomically smooth.

For grain coarsening or growth to occur by atomic attachment on atomically smooth interface, ledge generating sources such as 2-D

nucleation are necessary. When a disk shaped 2-D nucleus is assumed, the activation energy of nucleation, $\Delta G_{2\text{-}D}^{*}$, is given by[21]

$$\Delta G_{2-D}^{*} = \frac{\pi\varepsilon^2}{h\Delta G_v} \qquad (1)$$

where ε is the energy per unit length of edge, h is the height of nucleus and ΔG_v is the driving force for grain coarsening. Due to such an energy barrier for 2-D nucleation, only very large grains having enough driving force for coarsening can grow and lead to AGG.

For abnormally grown PMN-35PT grains in Fig. 1, reentrant edges were observed at the interfaces without exception. Note that the large grains marked *A* and *B* have butterfly and star-like shape, respectively. When single crystals are in thermodynamic equilibrium, they always exhibit convex planes. Therefore, the appearance of reentrant edges may indicate that the abnormal grain observed consists of several grains. However, grain boundaries inside the abnormal grain were not observed either by optical or by scanning electron microscopy. In order to answer this question, the crystallographic orientation of the grains was determined using EBSD.

Fig. 4 shows a specimen normal orientation map at the region of the grain marked *A* in Fig. 1. It reveals that the abnormal grain *A* consists mainly of two grains in contact with a very irregular grain boundary. Small grains trapped inside the large grain can also be discerned. Fig. 5 shows the distribution of the misorientation angles determined for the grain boundaries observed both inside and outside of the abnormal grain. The red color represents low angle boundaries (≤13°) and the blue represents high angle boundaries (≥41°). On the other hand, the yellow indicates the

grain boundaries with a misorientation between 14° and 40°.

The interesting features of the result shown in Fig. 5 are that all trapped grains have low angle boundaries and the zigzag boundary crossing the grain is a Σ3 coincidence site lattice (CSL) boundary. The Σ3 boundary is known to be formed by a 60 ° rotation about the <111> axis in a cubic crystal. Therefore, the Σ3 boundary is generally referred to as an incoherent twin boundary. For more than 20 abnormal grains examined, the same results were always obtained i.e. all the boundaries inside a large grain are either low angle or Σ3 boundaries.

When the solid grains dispersed in a liquid matrix impede each other during heat-treatment, they either maintain a liquid phase between them or form a grain boundary by exuding liquid. The higher the grain boundary energy, the higher the probability of liquid maintenance. In this respect, when the misorientation between the grains is small, they would coalesce with the formation of low angle grain boundaries of which energies are low. This will be the same for certain specific misorientations corresponding to the CSL boundaries, such as Σ3 in this experiment.

As schematically illustrated in Fig. 6 (a), grain coalescence results in the formation of reentrant edges. In the figure, reentrant angles, φ, of 134.8° and ~90° represent the Σ3 and low angle boundary, respectively. On the other hand, Fig. 6 (b) is the schematic illustration of 2-D nucleation at reentrant edges. In this case, the related force balance is

$$\gamma_{sl} = \gamma_{gb} + \frac{\varepsilon}{h}\cos\theta \qquad (2)$$

where γ_{sl} is the solid-liquid interface energy, γ_{gb} is the grain boundary

energy and θ is the contact angle of the nucleus. It implies that the lower the γ_{gb}, the lower the θ.

The 2-D nucleation at a reentrant edge shown in Fig. 6 (b) becomes easier with the decrease of the reentrant angle φ because the activation energy is proportional to the volume of nucleus.[22] When φ = 90°, the activation energy for nucleation is given as

$$G_{re}^{*} = G_{2-D}^{*} \frac{\theta - \sin\theta\cos\theta}{\pi} = G_{2-D}^{*} f(\theta) \qquad (3)$$

Note that ΔG_{re}^{*} is smaller than $\Delta G_{2\text{-}D}^{*}$ because $f(\theta)$ is always less than 1. For the 2-D nucleation process, in fact, even a 10 % reduction in activation energy can result in a hundredfold increase in the nucleation rate.[18] Therefore, the coarsening rate of a grain will be greatly enhanced when reentrant edges are present.

It can also be predicted from Eq. (2) and (3) that the nucleation rate becomes higher with the decrease in γ_{gb}. Note that the boundaries inside the abnormal grains are the low energy boundaries i.e. the low angle and Σ3 boundaries. In particular, the Σ3 boundary is an incoherent twin boundary with a very low boundary energy. Consequently, the reentrant edges formed by the Σ3 boundary will be the easiest nucleation sites leading to AGG. The presence of the Σ3 boundaries, without exception, in the abnormal grains may support this argument. Moreover, the Σ3 boundaries crossing the grain provide the permanent reentrant edges. The zigzag shape of the Σ3 boundary may suggest that nucleation and growth take place at both the planes of the reentrant edge by turns. On the other hand, the reentrant edges made by other low angle boundaries are transient

because they disappear with grain entrapment. In this respect, the Σ3 boundary in PMN-35 PT is believed to play a similar role as the (111) double twin in $BaTiO_3$. In BaTiO3, it has been reported that grains with twin plane reentrant edges (TPRE) due to (111) double twin grow extensively and result in AGG.[12-15]

IV. Conclusions

Abnormal growth of the PMN-35PT grains in PbO-rich liquid matrix was investigated. Through EBSD analysis, it was revealed that the abnormally grown large PMN-35PT grains did not exhibit a single crystal character. They are polycrystals composed of several grains. Only either low angle or Σ3 CSL boundaries are observed in the abnormal grain. The reentrant edges formed by such boundaries are suggested to cause AGG. In particular, the Σ3 boundaries are observed to play an important role for the AGG of PMN-35PT.

References

[1]S.-E. Park and T. R. Shrout, "Characteristics of Relaxor-Based Piezoelectric Materials for Ultrasonic Transducers," *IEEE Trans. Ulltraso., Ferroelectr. Frequency control*, Special Issue of Ultrasonic Transducers, **44** [5] 1140-47 (1997).

[2]S.-E. Park and T. R. Shrout, "Ultrahigh Strain and Piezoelectric Behavior in Relaxor Based Ferroelectric Single Crystals," *J. Appl. Phys.*, **82** [4] 1804-11 (1997).

[3]S. Nomura, T. Takahashi, and Y. Yokomizo, "Ferroelectric Properties in the System $Pb(Zn_{1/3}Nb_{2/3})O_3$ –$PbTiO_3$," *J. Phys. Soc. Jpn.*, **27**, 262 (1969).

[4]T. R. Shrout, Z. P. Chang, N. Kim, and S. Markgraf, "Dielectric Behavior of Single Crystals near the $(1-x)Pb(Mg_{1/3}Nb_{2/3})O_3$ –$(x)PbTiO_3$ Morphotropic Phase Boundary," *Ferroelectr. Letters*, **12**, 63-69 (1990).

[5]T. Li, A. M. Scotch, H. M. Chan, M. P. Harmer, S.-E. Park, T. R. Shrout, and J. R. Michael, "Single Crystals of $Pb(Mg_{1/3}Nb_{2/3})O_3$ –35 mol% $PbTiO_3$ from Polycrystalline Precursors," *J. Am. Ceram. Soc.*, **81** [1] 244-48 (1998).

[6]A. Khan, F. A. Meschke, T. Li, A. M. Scotch, H. M. Chan, and M. P. Harmer, "Growth of $Pb(Mg_{1/3}Nb_{2/3})O_3$–35 mol% $PbTiO_3$ Single Crystals from (111) Substrates by Seeded Polycrystal Conversion," *J. Am. Ceram. Soc.*, **82** [11] 2958-62 (1999).

[7]Y. J. Park, N. M. Hwang, and D. Y. Yoon, "Abnormal Growth of Faceted (WC) Grains in a (Co) Liquid Matrix," *Metall. Mater. Trans. A*, **27A**, 2809-19 (1996).

[8]S.-H. Rhee, J. D. Lee, and D.-Y. Kim, "Effect of Heating Rate on the Exaggerated Grain Growth Behavior of β-Si_3N_4," *Mater. Lett.*, **20**,115-20 (1997).

[9]Y.-W. Kim, J.-Y. Kim, S.-H. Rhee, and D.-Y. Kim, "Effect of Initial Particle Size on Microstructure of Liquid-Phase Sintered α-Silicon Carbide," *J. Eur. Ceram. Soc.*, **20** [7] 945-49 (2000).

[10]K. Choi, N.-M. Hwang, and D.-Y. Kim, "Effect of VC Addition on Microstructural Evolution of WC-Co Alloy: Mechanism of Grain Growth Inhibition," *Powder Metall.*, **43** [2] 197-201 (2000).

[11]S.-K. Kwon, S.-H. Hong, D.-Y. Kim, and N. M. Hwang, "Coarsening Behavior of Tricalsium Silicate (C_3S) and Dicalsium Silicate (C_2S) Grains Dispersed in a Clinker Melt," *J. Am. Ceram. Soc.*, **83** [5] 1247-52 (2000).

[12]M.-K. Kang, Y.-S. Yoo, D.-Y. Kim, and N. M. Hwang, "Growth of $BaTiO_3$ Seed Grains by the Twin-Plane Reentrant Edge Mechanism," *J.*

Am. Ceram. Soc., **83** [2] 385-90 (2000).

[13]M.-K. Kang, J.-K. Park, D.-Y. Kim, and N. M. Hwang, "Effect of Temperature on the Shape and Coarsening Behavior of $BaTiO_3$ Grains Dispersed in a SiO_2-rich Liquid Matrix," *Mater. Lett.*, **45**, 43-46 (2000).

[14]M.-K. Kang, D.-Y. Kim, H.-Y. Lee, and N. M. Hwang, "Temperature Dependence of the Coarsening Behavior of Barium Titanate Grains," *J. Am. Ceram. Soc.*, **83** [12] 3202-204 (2000).

[15]H.-Y. Lee, J.-S. Kim, N. M. Hwang, and D.-Y. Kim, "Effect of Sintering Temperature on the Secondary Abnormal Grain Growth of $BaTiO_3$," *J. Eur. Ceram. Soc.*, **20** [6] 731-737 (2000)

[16]S.-H. Lee, N. M. Hwang, and D.-Y. Kim, "Effect of Locally Presenting Anorthite Liquid on the Abnormal Grain Growth of Al_2O_3," *J. Eur. Ceram. Soc.*, in press.

[17]K.-S. Oh, J.-Y. Jun, D.-Y. Kim, and N. M. Hwang, "Shape Dependence of the Coarsening Behavior of Niobium Carbide Grains Dispersed in a Liquid Iron Matrix," *J. Am. Ceram. Soc.*, **83** [12] 3117-20 (2000).

[18]K. Choi, J.-W. Choi, D.-Y. Kim, and N. M. Hwang, "Effect of Coalescence on the Grain Coarsening during Liquid Phase Sintering of TaC-TiC-Ni Cermets," *Acta metall. mater.*, **48** [12] 3125-29 (2000).

[19]J.-J. Kim, B.-K. Kim, B.-M. Song, D.-Y. Kim, and D. N. Yoon, "Effect of Sintering Atmosphere on Isolated Pores During the Liquid-Phase Sintering of MgO-$CaMgSiO_4$," *J. Am. Ceram. Soc.*, **70** [10] 734-37 (1987).

[20]J.-H. Han and D.-Y. Kim, "Analysis of the Proportionality Constant Correlating the Mean Intercept Length to the Average Grain Size," *Acta metall. mater.*, **43** [8] 3185-88 (1995).

[21]J. P. Hirth and G. M. Pound, *Condensation and Evaporation*; p. 88. Progress in Materials Science, Vol. 11, Pergamon Press, U.K., 1963.

[22]D. A. Porter and K. E. Easterling, *Phase Transformations Metals and Alloys*; p.272. Chapman & hall, U.K., 1992.

List of Figures

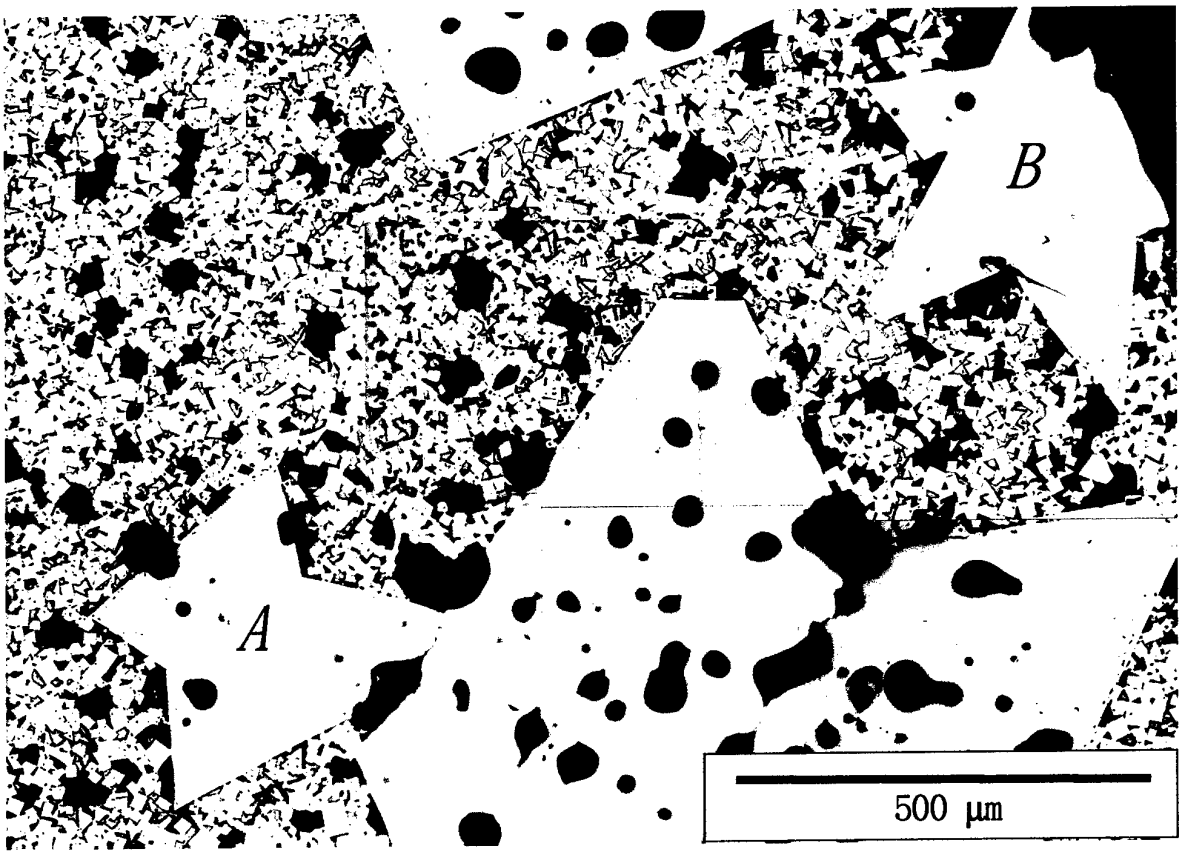

Figure 1. Optical micrograph of PMN-35PT with 10 mol% PbO heat-treated at 1200°C for 100 h.

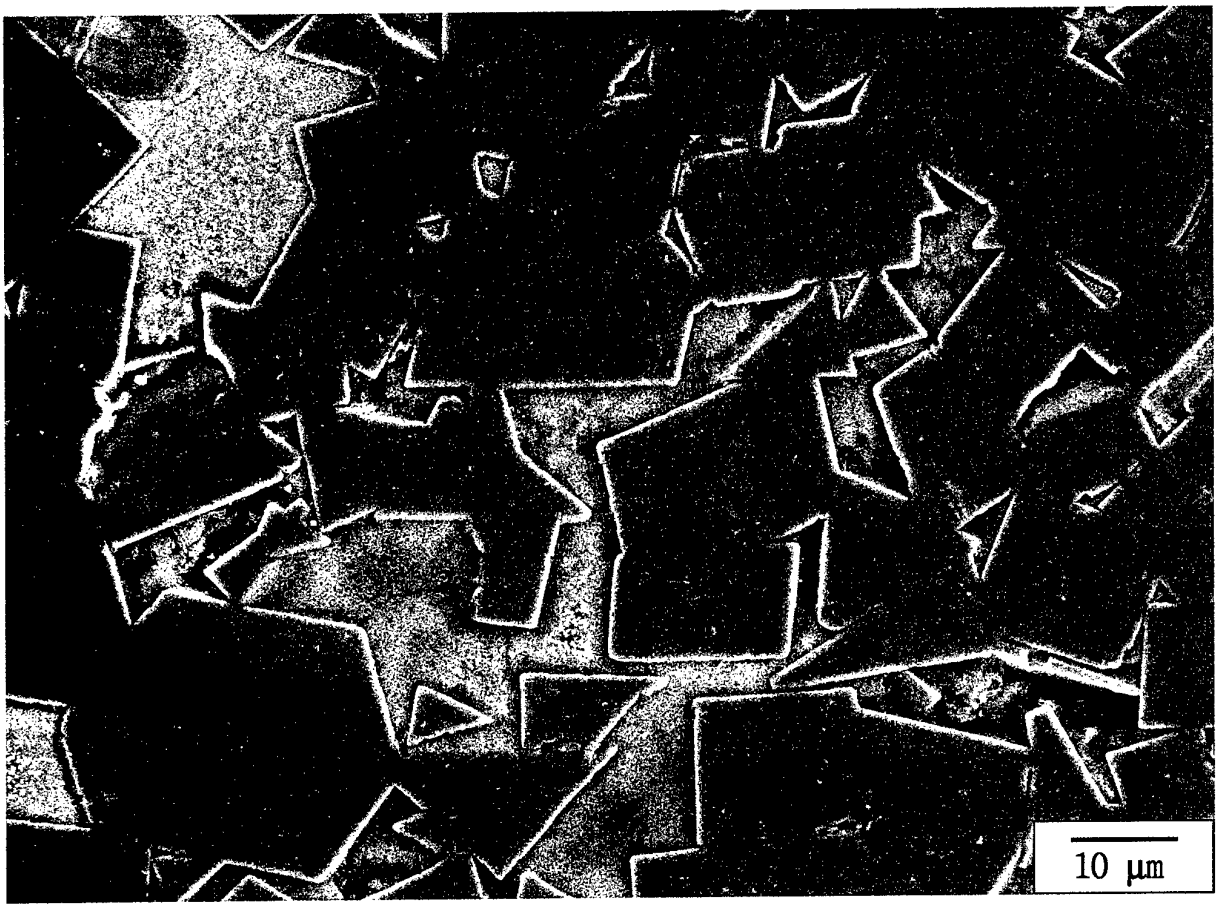

Figure 2. SEM micrograph of matrix grains of PMN-35PT with 10 mol% PbO heat-treated at 1200°C for 100 h.

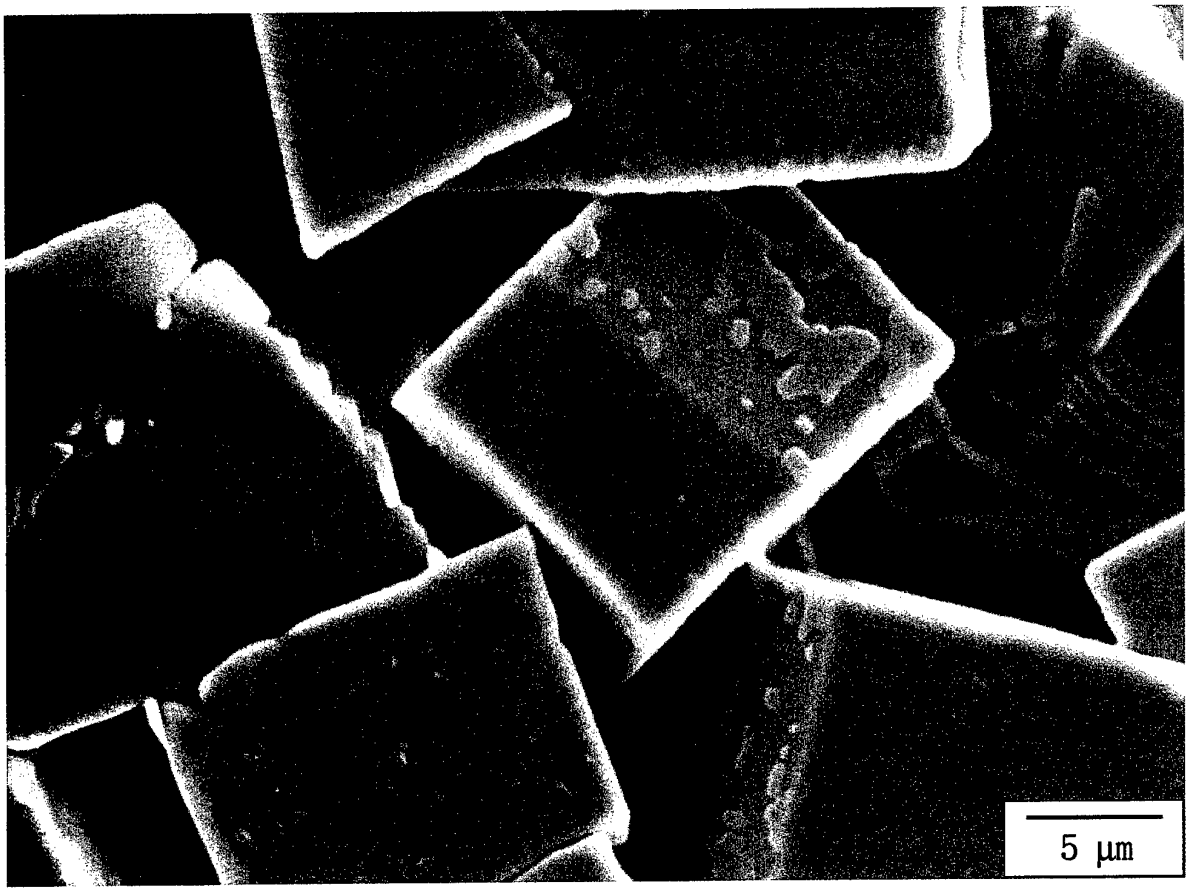

Figure 3. Three dimensional grain shape of PMN-35PT after leaching out liquid.

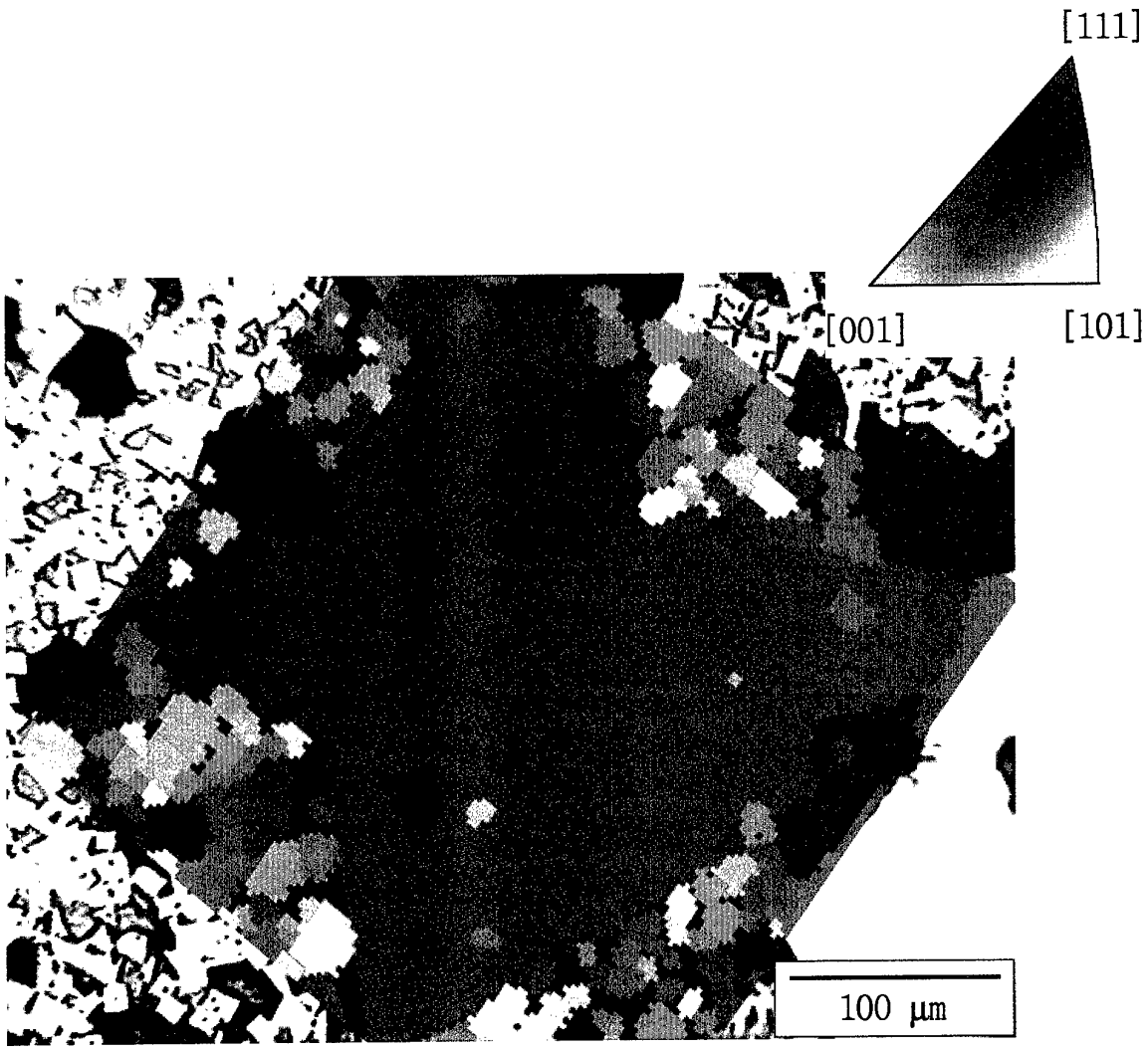

Figure 4. EBSD analysis result for the grain marked *A* in Fig. 1.

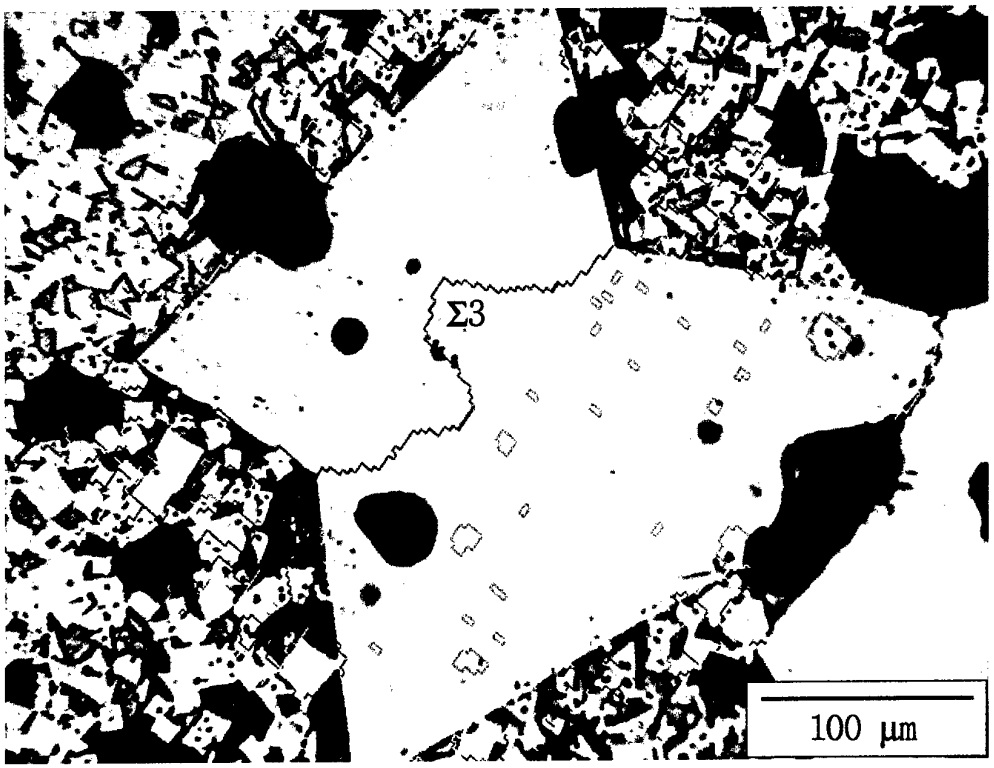

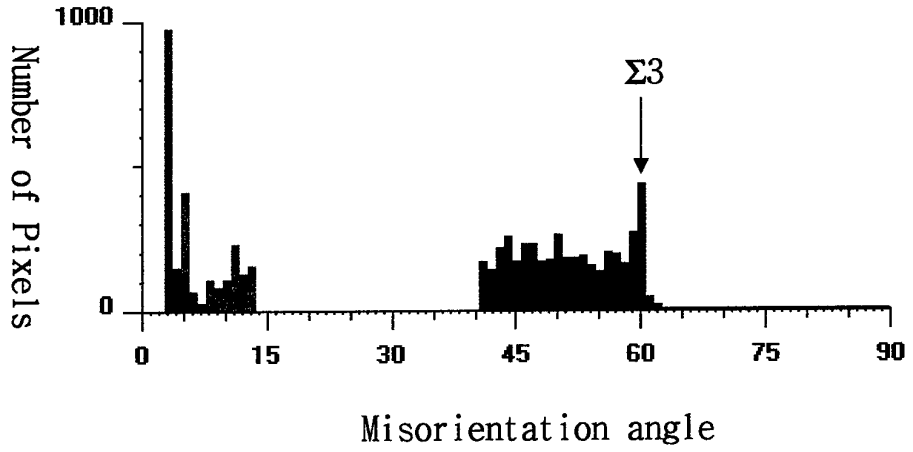

Figure 5. Distribution of grain boundary misorientation angles.

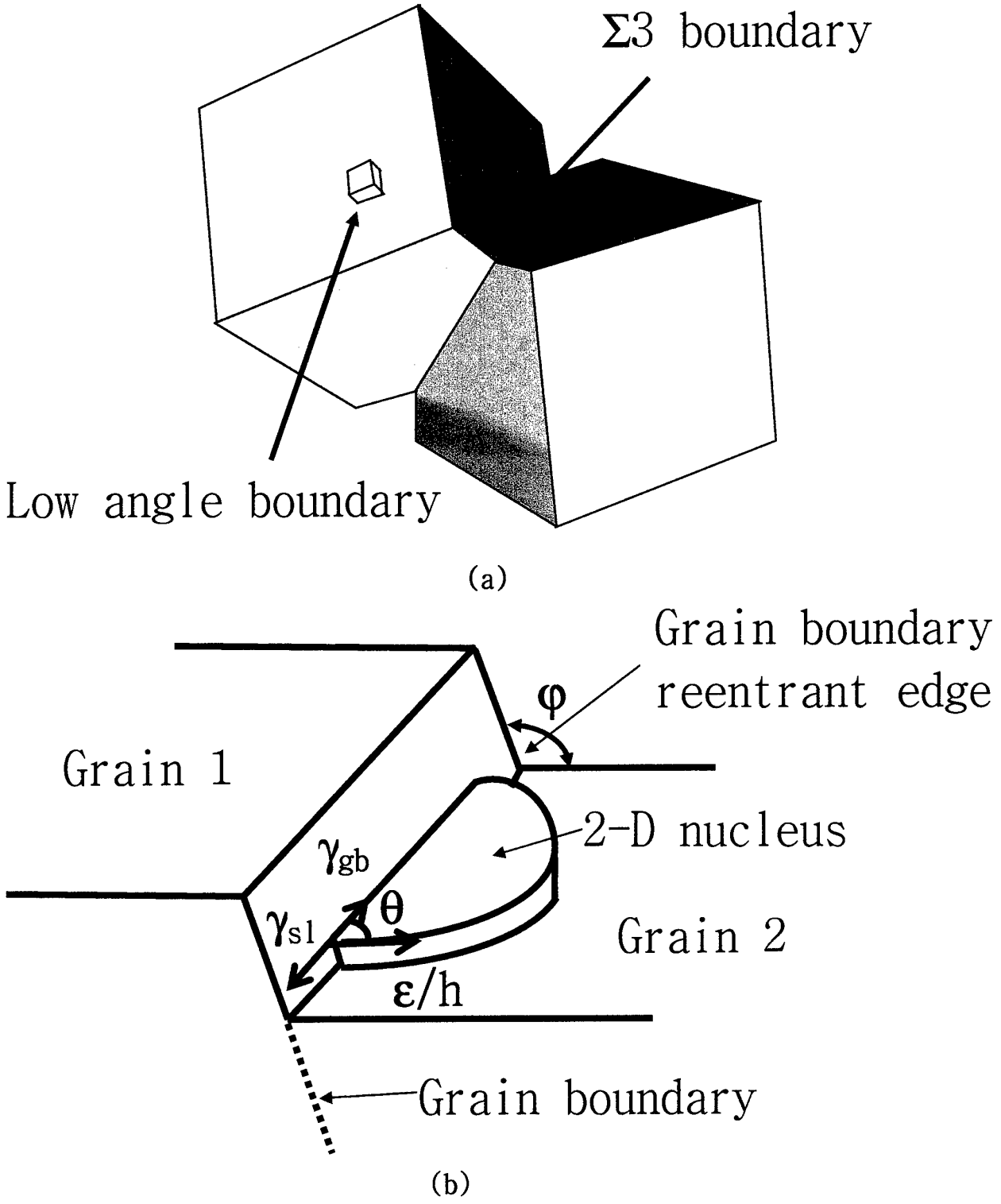

Figure 6. Schematic illustrations of (a) the grain coalescence and (b) 2-D nucleation at grain boundary reentrant edge.

Appendix 3

Preparation of Dense $Pb(Mg_{1/3}Nb_{2/3})O_3$ - $PbTiO_3$ Ceramics by Spark Plasma Sintering

Jong-Keuk Park[1,†], Ui-Jin Chung[1], Nong M. Hwang[2] and Doh-Yeon Kim[1]

[1]School of Materials Science and Engineering and Center for Microstructure Science of Materials, Seoul National Univ., Seoul 151-744, Korea and [2]Korea Research Inst. of Standards and Science, Daedok 305-600, Korea

---

Supported by the Ministry of Science & Technology of Korean Government through National Creative Research Initiatives and Asian Office of Aerospace Research and Development (AOARD-00-4003).

†Present address: Division of Thin Film Technology Research Center, Korea Institute of Science and Technology, Cheongryang 130-650, Seoul, Korea

Abstract

The effect of spark plasma sintering (SPS) on the densification behavior of $Pb(Mg_{1/3}Nb_{2/3})O_3$ - $PbTiO_3$ ceramics has been investigated. The specimens with a density higher than 99% of the theoretical were obtained by SPS treatment at 900℃. Through normal sintering at 1200℃, however, the density of the specimen was only about 92% of the theoretical.

I. Introduction

$Pb(Mg_{1/3}Nb_{2/3})O_3$ (PMN) and its solid solution with $PbTiO_3$ (PT) have been extensively investigated for various applications such as actuators and ultrasonic transducers.[1] When x=35 in PMN-xPT (x in mol%), the specimens are reported to be in the morphotropic phase boundary (MPB) and exhibit exceptional dielectric and piezoelectric properties.[2,3] However, it is difficult to obtain a fully dense PMN-35PT without a second pyrochlore phase. Even with the powders prepared by the columbite precursor method[4], both the pyrochlore phase and many pores remain after the low temperature sintering. On the other hand, a dense PMN-PT specimen is still difficult to obtain with high temperature sintering due to a PbO evaporation. In this case, excess PbO is usually added to compensate for the PbO loss and to enhance the material transfer by forming liquid phase during sintering.[5,6] However, such a PbO based liquid remaining at the grain boundaries is known to deteriorate the properties of PMN based ceramics.[7,8]

Compared to the conventional mixed oxide method, sol-gel[9] and oxalate method[10] are known to be effective for preparing fine PMN based powders, which enhance the density of a sintered specimen. Ando *et al.*[10] have reported that 96.7% of the theoretical density could be obtained for a PMN-10PT specimen after sintering at 900℃ with ~0.3 ㎛ diameter powders prepared by a modified oxalate method. On the other hand, Kwon *et al.*[11] have suggested that fully dense PMN-35PT ceramics could be achieved by reactive sintering at 1000℃ for 4 h in oxygen.

To obtain a fully dense and fine-grained material, spark plasma sintering (SPS) was introduced recently and has become widely used.[12-14] Although the mechanism of enhanced densification is not yet clearly understood, the process itself can be described quite simply: during sintering under relatively low pressure (~30MPa), a pulsed direct current, which generates spark discharge at the voids between the particles, is applied. Through the SPS process, a relatively low temperature and short sintering time (~ a few minutes) is sufficient to achieve full densification. In this investigation, therefore, the densification behavior of the PMN-35PT ceramics by SPS was studied. Dielectric and piezoelectric properties of the resultant PMN-35PT ceramics were also checked.

II. Experimental Procedures

PMN-35PT powders were prepared using the columbite precursor technique.[4] The $MgNb_2O_6$ precursor was prepared with MgO (High Purity Chemical Co., Sakado, Saitama, Japan > 99.9%) and Nb_2O_5 (Aldrich Chemical Co., Milwaukee, WI, U.S.A. > 99.9%). The powders were weighed and ball-milled for 24 h using a polyethylene jar with ethanol and zirconia balls. After drying, the powders were calcined at 1100℃ for 4 h in air. The PMN-35PT powders were then prepared with PbO (Aldrich Chemical Co., Milwaukee, WI, U.S.A. > 99.9%), TiO_2 (Aldrich Chemical Co., Milwaukee, WI, U.S.A. > 99.9%) and the $MgNb_2O_6$ obtained. Excess 0.5 mol% of PbO was added to the powder mixture. The powder mixture was again ball-milled. After drying, the powders were calcined at 850℃ for 4 h in air. The complete formation of perovskite was confirmed by X-ray diffraction analysis.

The powders were placed in a graphite die (8 mm in diameter) and heated to 900℃ under a uniaxial pressure of 30 MPa. The applied electric current during sintering was 1000 A and the heating rate was 400℃/min. After keeping for 5 min at 900℃, the electric current was stopped and the pressure was released. During SPS treatment, the specimens were slightly reduced so that they were annealed again in air at 800℃ for 2 h with $PbZrO_3$ powders. On the other hand, normal sintering as well as further heat-treatment of the specimen obtained by SPS was also carried out for a comparison. Green compacts pressed hydrostatically at 150 MPa were sintered at 1200℃ for 10 h. $PbZrO_3$ powders were also used as an atmospheric powder to prevent PbO evaporation. The heating rate was

5℃/min and the specimens were furnace-cooled.

The density of the specimens was measured using the Archimedes method in water. For microstructure observation using a scanning electron microscope (SEM), the cylindrical specimens were sectioned along the diameter and polished sections were thermally etched at 800℃ for 1 h. The average grain size was determined by multiplying 1.775 to the mean intercept length.[15] Dielectric and piezoelectric properties were determined by using disc type samples of 0.5-mm thick with flat and parallel surfaces. Silver pastes were painted on both sides of the samples, which were then heat-treated at 600℃ for 30 min. For low-field measurements using the IEEE resonance technique[16], samples were poled by field cooling (10kV/cm, 180~200℃) in a silicon oil bath. The temperature dependence of the dielectric constant was measured at 1kHz using an impedance analyzer (HP 4192A). The planar coupling factor (k_p), transverse coupling factor (k_{31}) and piezoelectric coefficient (d_{31}) were also measured by the resonance technique[16] using an impedance analyzer (Solartron 1260). The d_{33} value was determined by using a PIEZO d_{33} meter (MODEL ZJ-3D, Institute of Acoustics Academia Sinica).

III. Results and Discussion

Figure 1(a) and (b) show the microstructures, in two different magnifications, of a PMN-35PT specimen obtained by conventional sintering at 1200℃ for 10 h. The average grain size and density were measured to be 23.2 ㎛ and 7.48 g/cm^3 (92.0% of the theoretical density), respectively. Large pores up to ~40 μm were observed to distribute throughout the entire microstructure. In fact, such an insufficient densification of PMN-PT is an inherent problem. It can be due to high PbO vapor pressure, pore coalescence during sintering[17] and powder agglomeration. When the agglomerates are present in initial powders, large interagglomerate pores are reported to form at the initial stage of sintering since the densification of the agglomerates is much faster than that of the matrix.[18,19] Hereafter, this normally sintered specimen will be referred to as N-specimen.

Figure 2 is the microstructure of the specimen prepared by SPS at 900℃ for 5 min. Due to the low temperature and short sintering time, the microstructure consists of small grains. The average grain size was determined to be 1.1 ㎛. The pores are rarely observed throughout the entire microstructure. The density was measured to be 8.05 g/cm^3 (99.0% of the theoretical density). In order to compare this with the N-specimen (Fig. 1), the specimen prepared by SPS was further heat-treated at 1200℃ for 10 h, and its microstructure is shown in Fig 3, again in two different magnifications. During this subsequent heat-treatment, the density decreased slightly to 7.99 g/cm^3 (98.3% of the theoretical density) and the average grain size increased to 24.3 ㎛. Hereafter, the PMN-35PT

specimen prepared by SPS at 900℃ and subsequently heat-treated one will be referred to as the S- and SH-specimens, respectively.

Figure 4 shows the temperature dependence of the dielectric constant measured at 1kHz. The temperature of the maximum dielectric constant (T_m) was around 160℃ for both the N- and SH-specimen. The SH-specimen showed the highest peak value of 33,000, while that for the N-specimen was 28,000. For the S-specimen, however, T_m is measured to be 190℃. The dielectric constants around T_m are much lower than those of the N- and SH-specimens. Piezoelectric properties of the specimens are summarized in Table Ⅰ. As can be noted, the SH-specimen exhibited enhanced values of planar coupling factors (k_p), transverse coupling factors (k_{31}) and piezoelectric coefficients (d_{31}, d_{33}) compared to the other specimens. Since the SH- and N-specimens have almost same grain size, the property difference observed is mainly due to high density of the SH-specimen. Considering the highest density (99.0% of the theoretical density) of the S-specimen, however, the small grain sized material is definitely undesirable for dielectric and piezoelectric properties. The XRD analysis, by which we could detect no tetragonal phase in both S and SH specimens, support the grain size effect on the dielectric and piezoelectric properties. This has already been confirmed in the PMN and PMN-PT systems.[20,21] Note that the smaller the grain size, the larger the volume of less polarizable grain boundary phases.

IV. Conclusions

The SPS process is determined to be very effective for the densification of PMN-35PT ceramics. By SPS treatment at 900℃, a fully dense specimen was obtained. Specimens with a high-density and coarse grained microstructure could be obtained after the subsequent heat-treatment at 1200℃ for 10 h. For PMN-35PT, the higher the density and the larger the average grain size, the better the dielectric and piezoelectric properties are obtained.

V. References

1. K. Uchino, "Electrostrictive Actuators: Materials and Applications," *Am. Ceram. Soc. Bull.,* **65** [4] 647-52 (1986).
2. S. W. Choi, T. R. Shrout, S. J. Jang and A. S. Bhalla, "Dielectric and Pyroelectric Properties in the $Pb(Mg_{1/3}Nb_{2/3})O_3$-$PbTiO_3$ System," *Ferroelectrics,* **100** 29-38 (1989).
3. T. R. Shrout, Z. P. Chang, N. Kim and S. Markgraf, " Dielectric Behavior of Single Crystal near the $(1-x)Pb(Mg_{1/3}Nb_{2/3})O_3$-$(x)PbTiO_3$ Morphotropic Phase Boundary," *Ferroelectrics Letters,* **12** 63-69 (1990).
4. S. L. Swartz and T. R. Shrout, "Fabrication of Perovskite Lead Magnesium Niobate," *Mater. Res. Bull.,* **17** 1245-50 (1982).
5. Z.-G. Ye, P. Tissor, and H. Schmid, "Pseudo-Binary $Pb(Mg_{1/3}Nb_{2/3})O_3$–PbO Phase Diagram and Crystal Growth of $Pb(Mg_{1/3}Nb_{2/3})O_3$ [PMN]," *Mater. Res. Bull.,* **25** 739-48 (1990).
6. B. Jaffe, W. R. Cook, Jr., and H. Jaffe, *Piezoelectric ceramics*; p.117. Academic Press, London, U.K., 1971
7. H.-C. Wang and W. A. Schulze, "The Role of Excess Magnesium Oxide or Lead Oxide Determining the Microstructure and Properties of Lead Magnesium Niobate," *J. Am. Ceram. Soc.*, **73** [4] 825-32 (1990).
8. H. M. Jang, K.-M. Lee and M.-H. Lee, "Stabilization of Perovskite Phase and Dielectric Properties of $Pb(Zn,Mg)_{1/3}Nb_{2/3}O_3$-$PbTiO_3$ Ceramics Prepared by Excess Constituent Oxides," *J. Mater. Res.,* **9** [10] 2634-44 (1994).
9. P. Ravindranathan, S. Komarneni, A. S. Bhalla, and R. Roy, " Synthesis and Dielectric Properties of Solution Sol-Gel-Derived $0.9Pb(Mg_{1/3}Nb_{2/3})O_3$-$0.1PbTiO_3$ Ceramics," *J. Am. Ceram. Soc.,* **74** [12] 2996-99 (1991).
10. T. Ando, R. Suyama, and K. Tanemoto, "Preparation of $Pb(Mg_{1/3}Nb_{2/3})O_3$-$PbTiO_3$ Powder by a wet Chemical Process," *Jpn. J. Appl. Phy.,* **30** [4] 775-79 (1991).
11. S. Kwon, E. M. Sabolsky, and G. L. Messing, "Low-Temperature Reactive Sintering of 0.65PMN-0.35PT," *J. Am. Ceram. Soc.*, **84** [3] 648-50 (2001)
12. D. S. Perera, M. Tokita, and S. Moricca, "Comparative Study of Fabrication of Si_3N_4/SiC Composites by Spark Plasma Sintering and Hot Isostatic Pressing," *J. Eur. Ceram. Soc.,* **18** 401-04 (1998).
13. T. Takeuchi, M. Tabuchi, H. Kageyama and Y. Suyama, " Preparation of Dense $BaTiO_3$ Ceramics with Submicrometer Grains by Spark Plasma Sintering," *J. Am. Ceram. Soc.,* **82** [4] 939-43 (1999).
14. J. Hong, L. Gao, S.D.D.L. Torre, H. Miyamoto, and K. Miyamoto,

"Spark Plasma Sintering and Mechanical Properties of $ZrO_2(Y_2O_3)$-Al_2O_3 Composites," *Mater. Lett.*, **43** 27-31 (2000).
15. J.-H. Han and D. -Y. Kim, " Analysis of the Proportionality Constant Correlating the Mean Intercept Length to the Average Grain Size," *Acta Metall. mater.*, **43** [8] 3185-88 (1995).
16. "IRE standards on piezoelectric crystals: Measurements of piezoelectric ceramics, 1961", *Proc. IRE,* **49**, 1161-69 (1961).
17. U.-C. Oh, Y.-S. Chung, and D.-Y. Kim, " Effect of Grain Growth on Pore Coalescence During the Liquid –Phase Sintering of MgO-$CaMgSiO_4$ Systems," *J. Am. Ceram. Soc.*, **71** [10] 854-57 (1988).
18. K.-S. Oh, D.-Y. Kim, and S.-J. Cho, "Generation of Cracklike Voids during Sintering Al_2O_3-$10ZrO_2$ Ceramics and Their Prevention by Presintering with Low Pressure (2 MPa)," *J. Am. Ceram. Soc.*, **79** [6] 1723-25 (1996).
19. J.-W. Son, D.-Y. Kim, and P. Boch, "Enhanced Densification of In_2O_3 Ceramics by Presintering with Low Pressure (5 MPa)," *J. Am. Ceram. Soc.*, **81** [9] 2489-92 (1998).
20. P. Papet, J. P. Dougherty, and T. R. Shrout, "Particle and Grain Size Effects on the Dielectric Behavior of the Relaxor Ferroelectric $Pb(Mg_{1/3}Nb_{2/3})O_3$," *J. Mater. Res.*, **5** [12] 2902-09 (1990).
21. T. R. Shrout, U. Kumar, M. Megherhi, N. Yang, and S.-J. Jang, " Grain Size Dependence of Dielectric and Electrostriction of $Pb(Mg_{1/3}Nb_{2/3})O_3$–Based Ceramics," *Ferroelectrics,* **76** 479-87 (1987).

Table I. Piezoelectric properties of the specimens obtained.

	k_p	k_{31}	d_{31} (pc/N)	d_{33} (pc/N)	K_{max} (1kHz)
N-specimen	0.495	0.291	-178	500	28,000
S-specimen	0.161	0.095	-38	85	5,000
SH-specimen	0.634	0.372	-241	590	33,000

List of figure captions.

Fig. 1 Microstructures of a typical PMN-35PT specimen sintered at 1200°C for 10 h; (a) polished surface and (b) thermally etched surface.

Fig. 2 Microstructure of a typical PMN-35PT specimen prepared by SPS at 900°C.

Fig. 3 Microstructures of a typical PMN-35PT specimen prepared by SPS and then heat-treated at 1200°C for 10 h; (a) polished surface and (b) thermally etched surface.

Fig. 4. Variation of the dielectric constant with temperature for the PMN-35PT specimens.

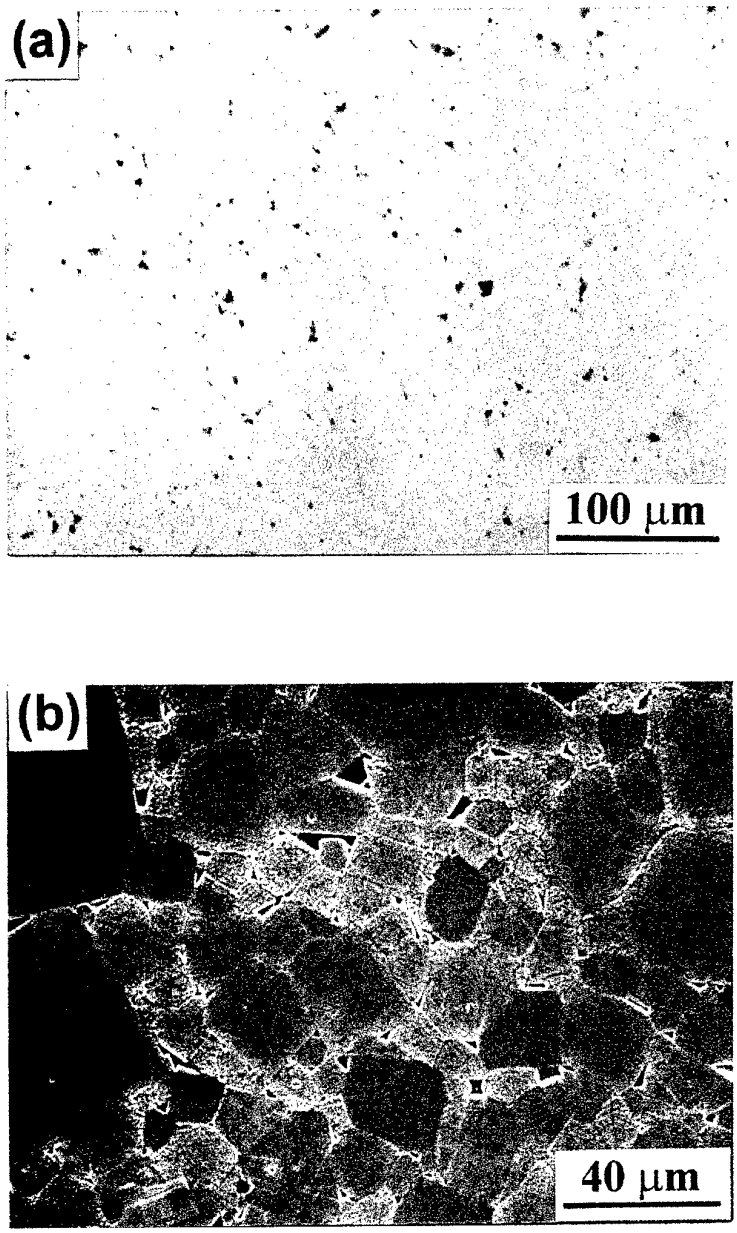

Fig. 1 Microstructures of a typical PMN-35PT specimen sintered at 1200°C for 10 h; (a) polished surface and (b) thermally etched surface.

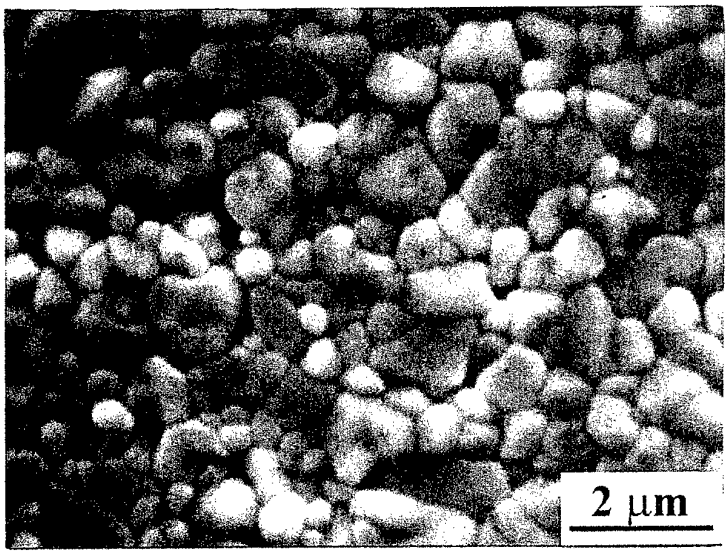

Fig. 2 Microstructure of a typical PMN-35PT specimen prepared by SPS at 900°C.

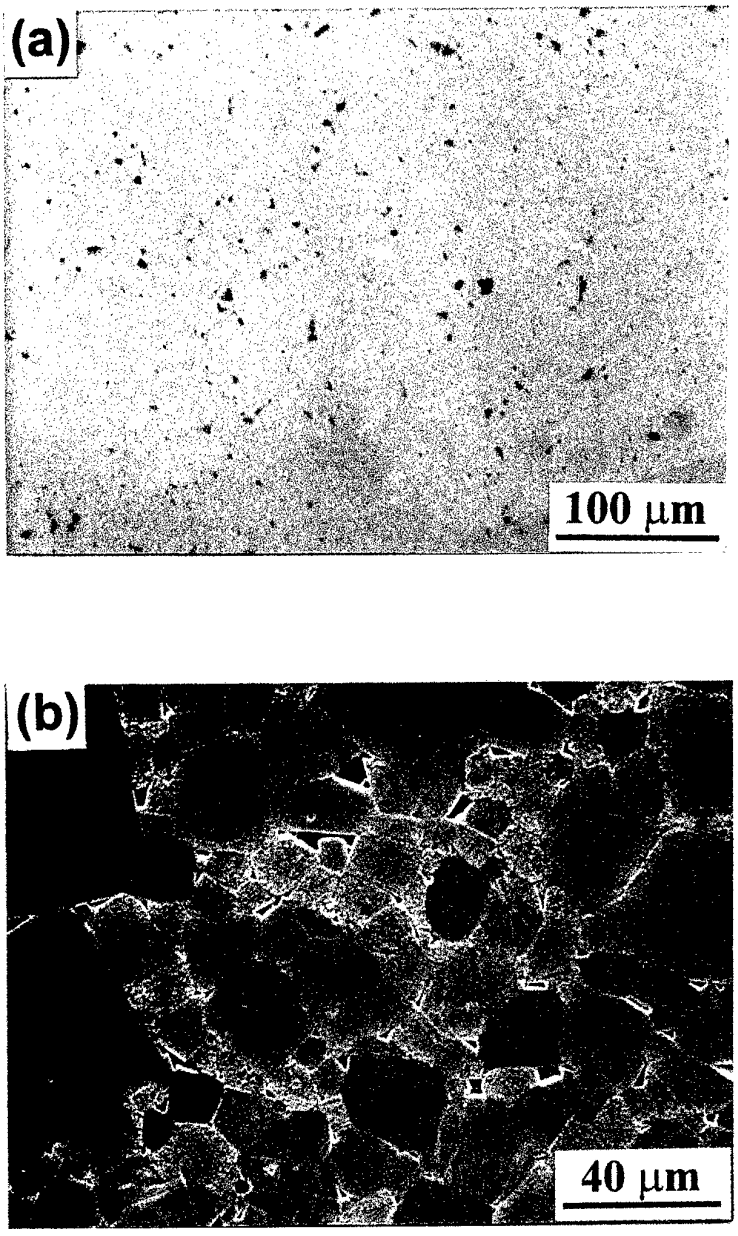

Fig. 3 Microstructures of a typical PMN-35PT specimen prepared by SPS and then heat-treated at 1200°C for 10 h; (a) polished surface and (b) thermally etched surface.

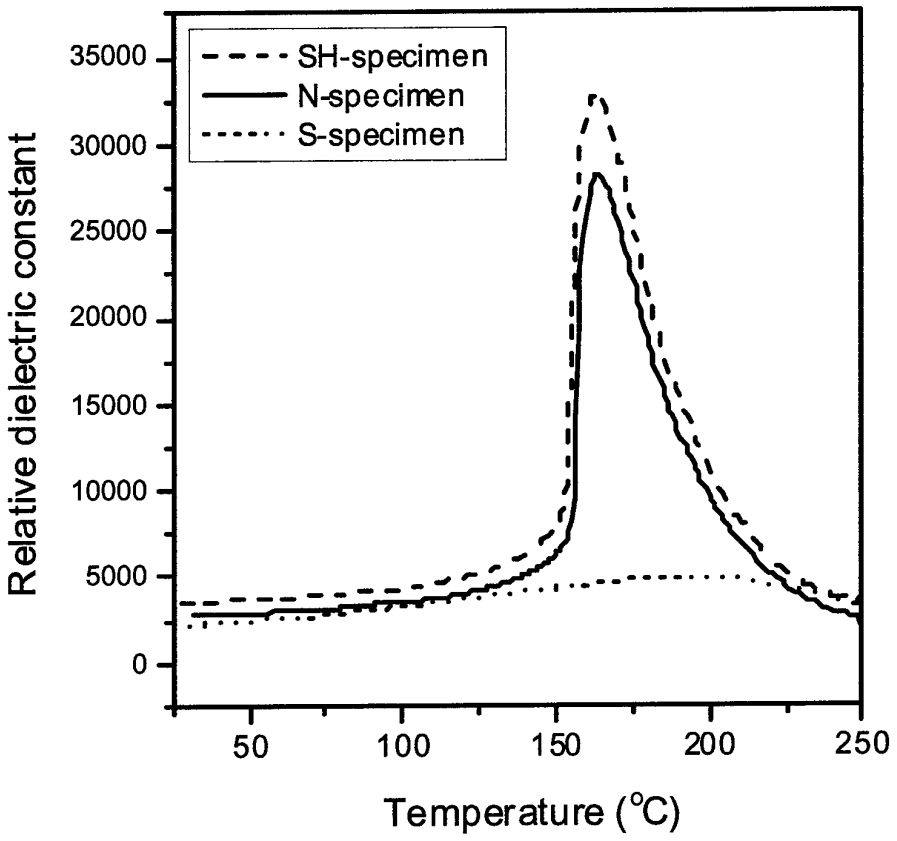

Fig. 4. Variation of the dielectric constant with temperature for the PMN-35PT specimens.